GLOBAL SOLAR ATLAS 2.0

VALIDATION REPORT FOR GLOBAL SOLAR RADIATION MODEL

November 2019

This report was prepared by Solargis, under contract to the World Bank.

It is a deliverable from the activity "Global Solar Atlas" [Project ID: P161130], and therefore relates to the solar resource database available via the Global Solar Atlas. This activity was funded and managed by the Energy Sector Management Assistance Program (ESMAP), a multi-donor trust fund administered by the World Bank, under a global initiative on Renewable Energy Resource Mapping. Further details on the initiative can be obtained from the ESMAP website.

The content of this document is the sole responsibility of the consultant authors.

Washington, DC 20433, USA
Telephone: +1-202-473-1000
Internet: www.worldbank.org

Disclaimer

Rights and Permissions

Attribution

Please cite the work as follows: ESMAP. 2019. Validation Report for Global Solar Radiation Model. Washington, DC: World Bank.

Solar Resource Database

Validation of Solargis solar radiation model

Reference No. 170-11/2019
Date: 29 November 2019

Customer:

The World Bank
Contact: Mr Oliver Knight
Address: 1818 H Street, N.W.,
Washington, DC 20433, USA
Tel. +421249212491
E-mail: oknight@worldbank.org
https://globalsolaratlas.info

Consultant:

Solargis s.r.o.
Contact: Mr. Marcel Suri Address:
Mytna 48
811 07 Bratislava, Slovakia
Tel. +421 2 4319 1708
E-mail: marcel.suri@solargis.com
https://solargis.com

Revision record

Revision	Date	Edited	Approved	Description
-	29 Nov 2019	All	Marcel Suri	Original document

TABLE OF CONTENTS

1 Summary ... 6
1.1 Background ... 6
1.2 Data and methods ... 6
1.3 Results ... 6
2 Introduction ... 7
2.1 Solar terminology and parameters ... 7
2.2 How to acquire solar data: measurements vs. models ... 7
2.3 Solargis data for all stages of a PV project ... 9
3 Solargis solar resource database ... 10
3.1 Key features ... 10
3.2 Solargis calculation scheme ... 12
4 Accuracy of Solargis ... 16
4.1 Indicators of model accuracy ... 16
4.2 Ground measurements requirements ... 16
4.3 Representativeness of validation sites ... 17
4.4 Model validation: Bias ... 18
4.5 Model validation: Root mean square deviation ... 21
5 Uncertainty of solar model: yearly estimates ... 23
5.1 Simplified characterization of bias distribution ... 23
5.2 Identification of main situations with low and high uncertainty levels ... 25
5.3 Advanced analysis of factors affecting solar model uncertainty ... 25
6 Independent validation studies ... 27
7 Conclusions ... 28
8 Acronyms ... 29
9 Glossary ... 31
10 List of figures ... 33
11 List of tables ... 34
12 References ... 35
13 Support information ... 37
13.1 Background on Solargis ... 37
13.2 Legal information ... 37
14 Annex ... 38
List of validation sites ... 38
GHI validation statistics ... 45
DNI validation statistics ... 52

1 SUMMARY

1.1 Background

The work is funded by the Energy Sector Management Assistance Program (ESMAP), administered by The World Bank and supported by bilateral donors. ESMAP is a partnership between the World Bank Group and its 18 partners to help low- and middle-income countries reduce poverty and boost growth, through environmentally sustainable energy solutions. ESMAP initiative on Renewable Energy Resource Mapping includes assessment and mapping of biomass, small hydro, solar and wind.

This technical report shows method and results of validation of solar resource model developed and operated by Solargis. Validation of the solar model has been performed using data from professional public networks of ground measurement stations worldwide, and also solar measurements acquired within the measurement campaigns run in countries, sponsored by the World Bank, the ESMAP initiative (https://globalsolaratlas.info/solar-measurement).

1.2 Data and methods

This report documents validation of solar resource data calculated by Solargis satellite model. Chapter 2 provides introduction to the topic of solar resource, the measurement approaches and solar models. Short description of the solar model principles, characteristics of input satellite and atmospheric data as well as key features of the Solargis model outputs is summarized in Chapter 3.

The validation of model is based on ground measurements from 228 public stations (Chapter 4). The stations are located in various climate zones and give comprehensive information of model performance in different conditions.

The validation results show consistent model performance globally for various geographic conditions. The validation findings are in Chapter 5 generalised into the uncertainty of the Solargis model data. Factors affecting the uncertainty are outlined, and typical uncertainty ranges are given.

1.3 Results

Validation demonstrates reliable performance of Solargis model globally. The validation and previous experience indicate that with using of high-quality local measurements the Solargis model output has further potential for reduction of uncertainty, especially in tropical climate.

2 INTRODUCTION

2.1 Solar terminology and parameters

Solar resource availability determines how much electricity will be generated in a given time. Analysis of the solar radiation components makes it possible to understand the performance of solar power plants (Table 2.1).

From the terminology point of view it is to be noted that while solar **irradiance** refers to solar power (instantaneous energy) falling on a unit area per unit time [W/m^2], solar **irradiation** is the amount of solar energy falling on a unit area over the given time interval [Wh/m^2 or kWh/m^2]. Solargis offers solar irradiation and irradiance, depending on a data product.

Table 2.1: Solar resource parameters provided by Solargis to solar power industry

Parameter	Acronym	Description	Unit
Global Horizontal Irradiance (Irradiation)	GHI	Sum of diffuse and direct (transposed on horizontal surface) components. It is considered as a climate reference as it enables comparing individual sites or regions	W/m^2 for irradiance Wh/m^2 or kWh/m^2 for irradiation
Direct Normal Irradiance (Irradiation)	DNI	Component that directly reaches the surface, and is relevant for concentrating solar thermal power plants (CSP) and photovoltaic concentrating technologies (CPV)	
Diffuse Horizontal Irradiance (Irradiation)	DIF	Part of the irradiation that is scattered by the atmosphere. Higher values of DIF/GHI ratio represent higher occurrence of clouds, higher atmospheric pollution or higher water vapour	
Global Tilted Irradiance (Irradiation)	GTI	Sum of direct and diffuse solar radiation falling on a tilted surface. Unlike the horizontal surface, the tilted surface also receives small amount of ground-reflected radiation. It determines performance characteristics of photovoltaic (PV) technology.	

2.2 How to acquire solar data: measurements vs. models

The quality of solar resource data is critical for economic and technical assessment of solar power plants. Understanding uncertainty and managing weather-related risk is essential for successful planning and operating of solar electricity assets. High quality solar resource and meteorological data are available today, and they can be obtained by two approaches:

- By diligent operation of **high-accuracy solar instruments** installed at a meteorological station. Well-maintained solar instruments offer higher accuracy and high-frequency data for a given site. Typically, such data is available only for limited period of time, from few months to few years. The number of high-quality solar measuring stations, deployed worldwide, is relatively limited and sparsely distributed in certain regions. If not maintained properly, the measurements may suffer from insufficient cleaning, misalignment, miscalibration, errors in data logger and transfer and other operational issues.
- By complex **solar meteorological models** that read satellite, atmospheric and meteorological data as inputs. Such models are typically less accurate, compared to the good quality measurements. But their advantage is continuous geographical coverage, and ability to serve data for any location with a continuous history of 12 to 25 recent years. The model data is relatively stable and not affected to the kind of operational instability issues as typical for the ground instruments. Advantage of the models is also their ability to serve data in real time for monitoring and forecasting. To achieve high reliability and low uncertainty, these models are calibrated and validated using high quality ground measurements.

Solargis represents the latter (modelling approach), based on the use of modern and verified solar algorithms. The model offers long and continuous history and systematic update of primary solar resource parameters (GHI and DNI) as well as all derived parameters and data products needed by solar energy industry.

Table 2.2: Comparing solar measurements and model data

	Ground-measurements	Data from solar models
Availability/ accessibility	Available only for limited number of locations Data cover various time periods of time: from several months to years Difficult to access and use	Data are available for any land location Data cover long period of time (at present 12 to 25 years) Data are prepared in a standardised format for easy use
Original spatial resolution	Local measurement representing microclimate with all local weather occurrences	Regional simulation, representing regional weather patterns with grid resolution of recently available data inputs from 90 metres (terrain), 3 km (clouds), to 50-100 km (aerosol). Therefore the local values are slightly smoothed with missing
Original time resolution	Typically, 1-minute readings are used. Data is often aggregated to 5- or 10-minute values. Aggregation to one hour is also used.	Modern satellites: 10 and 15 minutes Historical satellites: 30 minutes
Quality	Before any use, data need to go through rigorous quality control and possibly also gap filling.	Automated quality control functions are used to monitor the input data, computation and data delivery. This enables delivery of stable outputs with predictable quality.
Completeness of data set	A number of missing or incorrect values is typically detected during quality control	Missing records are very rare in the modern satellite and model data inputs. Intelligent gap-filling algorithms are used for gap filling. Historical satellite missions show higher percentage of missing or incorrect data records.
Stability	Sensors, measuring practices, maintenance and calibration may change over time, as well as the operation and maintenance practices. Thus long term stability is typically a challenge.	Historical time series data is calculated with one single and stable model. Data for operational (real-time) services are computed by operational models and data inputs that may differ from the stable models and data inputs. Therefore, re-computation takes place within 2 days of delivery (for real time data) and after each month for historical data.
Uncertainty	Uncertainty is related to the accuracy category and maintenance of sensors, yet the main component of uncertainty are the operation and maintenance practices and data management and quality control. The measurement data represent the very local solar microclimate conditions, which renders their use within the larger territory very limited.	Uncertainty is given by the resolution of input data and quality of the computation model. For the case of high frequency values (minute, hourly, daily values) the uncertainty may be higher for models when compared to calibrated and well-maintained high-accuracy ground sensors. For monthly and yearly aggregated values, the uncertainty of model outputs is comparable to good quality measurements. The model data represent the regional solar climate, namely when it regards the effect of clouds, water vapour and aerosols. Yet the shading of terrain is represented by the terrain data inputs calculated at spatial resolution of 90 x 90 metres (Prospect web app) and 250 x 250 metres (in time series and TMY).

Solar parameters retrieved from satellite-based model have lower spatial and temporal resolution compared to on-site solar measurements. Unlike measurements, the solar model represents regional climate patterns (mainly given by resolution of satellite data) rather than local microclimate. This means that especially high frequency values (e.g. in 1-minute measurements) are rather smoothed and not well represented in the occurrence statistics.

2.3 Solargis data for all stages of a PV project

Technically, good solar resource data should meet the following criteria:

- Computation should be based on scientifically proven methods
- Outputs should be systematically validated and traceable
- Data should represent at minimum 10 years of harmonized history, optimally 25 year or more
- Data should be available fast and for any location
- Outputs should include information about solar resource uncertainty
- Data should be supported by an analytical technical report with metadata
- Service should be supported by dedicated professional team of experts

Solargis database is designed to help effective development of solar energy strategies and projects at all stages of their lifetime, i.e. for:

- **Prospection**: strategical planning, site identification, and prefeasibility of projects
- **Evaluation**: technical design, financial and technical due diligence
- **Monitoring**: systematic site evaluation, performance assessment and asset management
- **Forecasting**: for optimised management of power production, balancing, and energy trade

Solargis database is a product of 19 years of dedicated research and development. At present the solar resource database covers land territories between latitudes 60N and 55S (in Latin America to 45°S). Solargis database incorporating a number of unique and innovative features:

- All models have been developed and adapted by Solargis – to provide harmonized performance of solar model with the other atmospheric, meteorological and geographical data
- Computed by the best available methods and input data sources, continuously improved and adapted to new data inputs and challenges
- High quality and reliability, systematically monitored and quality controlled
- Time series are computed at high temporal and spatial resolution (10 and 15-minute data, respecting the terrain shading up to 90 metres)
- Models are adapted, calibrated and validated at more than 1000 ground measurements worldwide, to operate in a stable and predictable way in all climate patterns and geographies
- The data represent a long history (up to 25 years) and it is updated globally in real time
- The models are continuously validated by Solargis and by external organizations.

3 SOLARGIS SOLAR RESOURCE DATABASE

3.1 Key features

Solargis database is organised in segmented data files that include grid (raster) data layers structured for a given period of time. Table 3.1 shows technical features of Solargis solar resource data. Temporal coverage varies by region and the variability is given by historical availability and features of different satellite missions. At present, we are processing data from three meteorological data centres operating geostationary satellites at five key positions that cover by data entire Earth (valid data is not available for polar regions). See Chapter 3.2 for the model calculation scheme.

Table 3.1: Solargis solar resource data: Summary of technical features

Parameters	Description
Spatial coverage	Land surface and coastal seas between latitudes 60°N to 45°S
Time representation	Time series since 1994/1999/2006 depending on the satellite region (Figure 3.1)
Spatial (grid) resolution	Primary data resolution 2 to 6 km (Table 3.3) Enhanced resolution by downscaling: - ~90 m for time series and TMY - ~250 m for Global Solar Atlas and Solargis Prospect
Temporal resolution (time step)	Primary time series: 10/15/30 minutes depending on the satellite region and historical operation Derived data products: - Aggregated into hourly, daily, monthly and yearly values - Synthetically generated solar resource data: 1-minute step

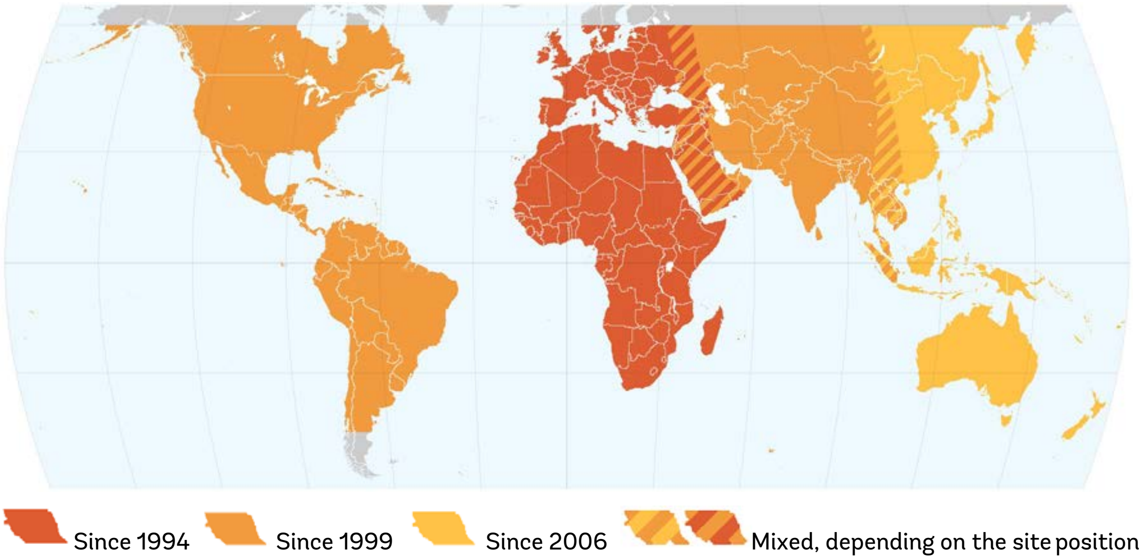

Figure 3.1: Historical data availability

Figures 3.2 and 3.3 show geographic distribution of long-term yearly sums of solar radiation worldwide. The maps show aggregated values of Solargis historical database for land territories.

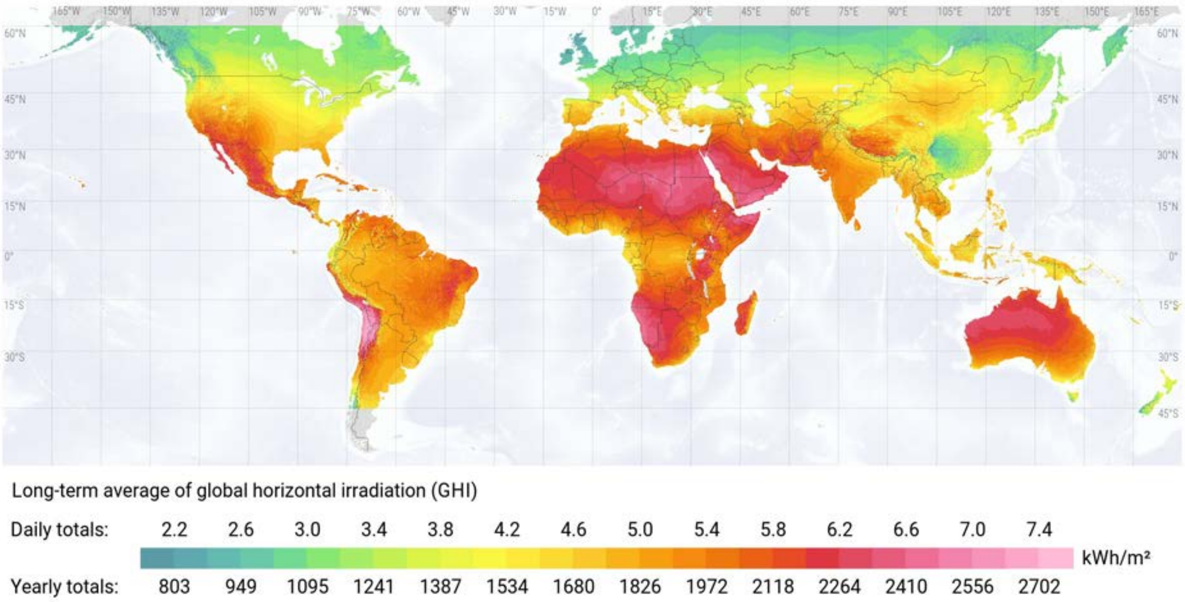

Figure 3.2: Global Horizontal Irradiation: Long term yearly average or daily/yearly summaries

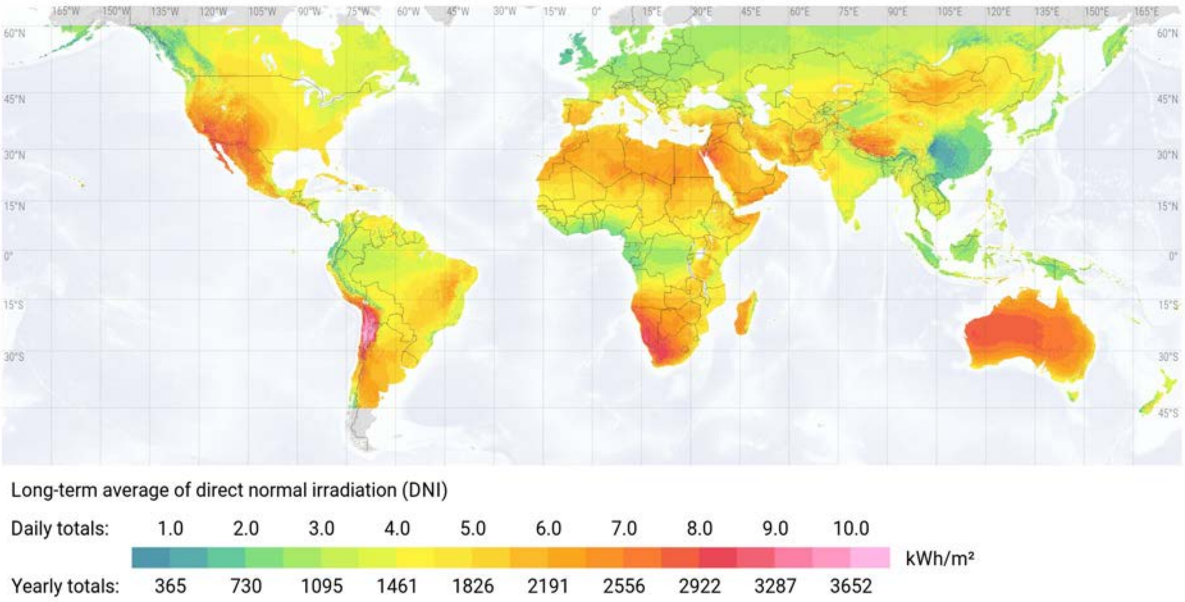

Figure 3.3: Direct Normal Irradiation: Long term yearly average or daily/yearly summaries

3.2 Solargis calculation scheme

The solar radiation retrieval in Solargis is fundamentally split into three steps. First, the **clear-sky irradiance** (the irradiance reaching ground with assumption of absence of clouds) is calculated using the clear-sky model. Second, the satellite data is used to quantify the attenuation effect of clouds by means of **cloud index** calculation. Then, the clear-sky irradiance is coupled with cloud index to retrieve **all-sky irradiance**. This process is represented in Figure 3.4. A comprehensive **overview of the Solargis model** is made available in the book publication [2]. The methodology is also described in [3, 4].

The outcome of the procedure is direct normal and global horizontal irradiance, which is used for computing diffuse and global tilted irradiance. The data from satellite models are usually further post-processed to get irradiance that fits the needs of specific applications (such as solar irradiance on tilted or tracking surfaces) and/or solar irradiance corrected for shading effects from surrounding terrain orobjects.

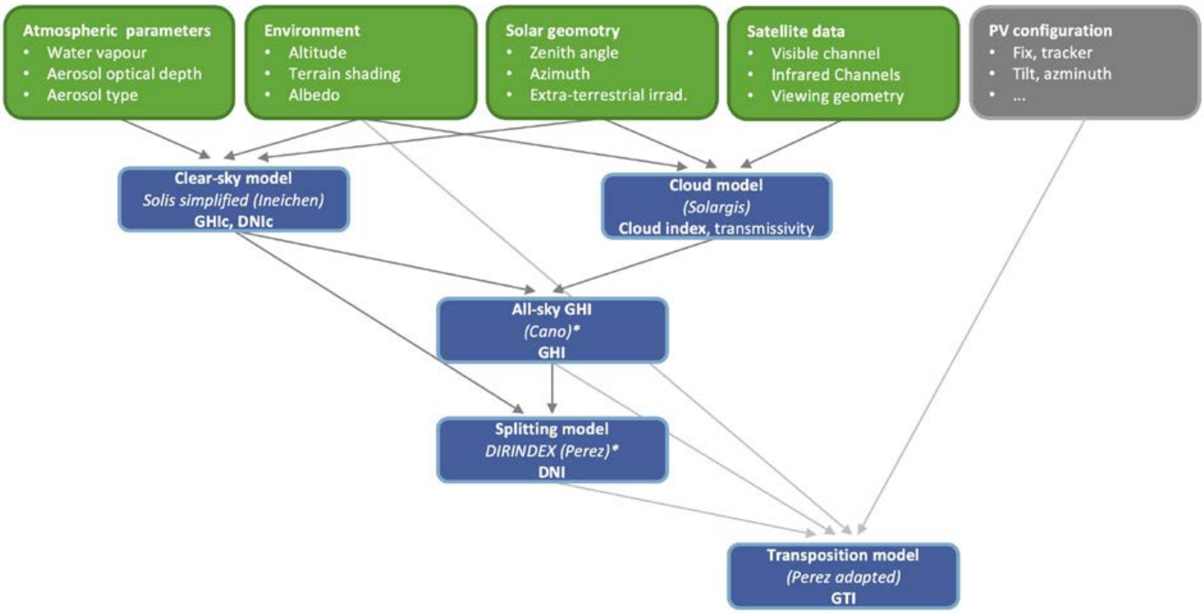

Figure 3.4: Scheme of the semi-empirical solar radiation model (Solargis)

Clear-sky model simplified SOLIS [5] calculates clear-sky irradiance from a set of input parameters. Sun position is a deterministic parameter, and it is described by algorithms with good accuracy. Three constituents determine geographical and temporal variability of clear-sky atmospheric conditions:

- **Aerosols** are represented by Atmospheric Optical Depth (AOD), which is derived from the global MERRA-2 and MACC-II/CAMS databases [6, 7, 8]. The model uses daily variability of aerosols to simulate more precisely the instantaneous estimates of DNI and GHI [9, 10]. Use of daily values reduces uncertainty, especially in regions with variable and high atmospheric load of aerosols.
- **Water vapour** is also highly variable, but compared to aerosols, it has lower impact on magnitude of DNI and GHI change. The daily data are derived from CFSR and GFS databases for the whole historical period up to the present time [11, 12, 13].
- **Ozone** has negligible influence on broadband solar radiation and in the model, it is considered as a constant value.

Cloud model estimates cloud attenuation on global irradiance. Data from meteorological geostationary satellites are used to calculate a cloud index that relates radiance of the Earth's surface, recorded by the satellite in several spectral channels with the cloud optical transmittance. In Solargis, the modified calculation scheme by Cano has been adopted to retrieve cloud optical properties from the satellite data [14]. A number of improvements are introduced to better cope with complex identification of albedo in tropical variable cloudiness, complex terrain, at presence of snow and ice, etc. Other support data are also used in the model, e.g. altitude and air temperature.

To calculate **Global Horizontal Irradiance** (GHI) for all atmospheric and cloud conditions, the clear-sky global horizontal irradiance is coupled with cloud index.

From GHI, other solar irradiance components (direct, diffuse and reflected) are calculated. **Direct Normal Irradiance** (DNI) is calculated by modified Dirindex model [15]. Diffuse horizontal irradiance is derived from GHI and DNI.

Calculation of **Global Tilted Irradiance (GTI)** from GHI deals with direct and diffuse components separately. While calculation of direct component is straightforward, estimation of diffuse irradiance for a tilted surface is more complex and affected by limited information about shading effects and albedo of nearby objects. For converting diffuse horizontal irradiance for a tilted surface, the adapted Perez transposition model is used [16]. Reflected component is also approximated considering that knowledge of local conditions is limited.

Model for simulation of **terrain** effects (elevation and shading) based on high resolution altitude and horizon data. Model by Ruiz Arias [17] is used to achieve enhanced spatial representation – from the resolution of satellite (2 to 3 km at the subsatellite point) to the resolution of digital terrain model (90 metres in Prospect app and 250 metres in the delivery of time series and TMY).

A description of model inputs can be found in Table 3.2. Considering the shading from terrain, the spatial resolution of data products is enhanced up to 3 arc-seconds (which is about 90 metres at the equator, less towards the poles). Typically, SRTM3 elevation data is used for this operation. Final data can be recalculated to any other spatial resolution.

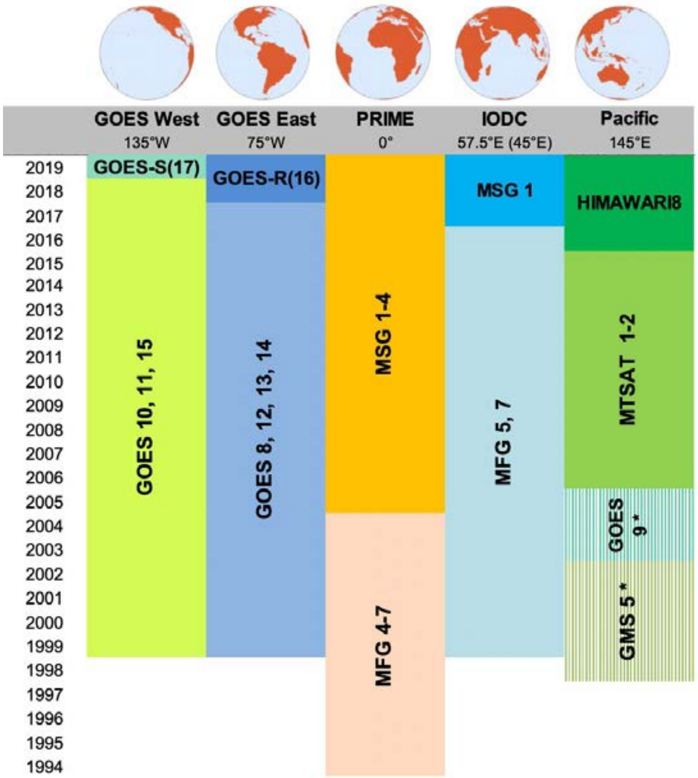

Figure 3.5: Satellite missions used for cloud identification
(GMS 5 and GOES 9 satellites experience failures and these data are not used in the processing)

Primary time step of solar resource parameters is 15 minutes for Meteosat MSG satellites, 30-minutes for Meteosat MFG, MTSAT and GOES East and West satellites and 10-minutes for GOES R (part of GOES R archive has 15-minute time step), GOES S and Himawari satellites. Atmospheric parameters (aerosols and water vapour) represent daily data.

Spatial resolution of Meteosat, GOES, and PACIFIC data considered in the calculation scheme is approximately 2.5 km to 4 km at sub-satellite point (more details in Table 3.3). Model outputs are resampled to 2 arc-minutes (app. 4x4 km) regular grid in WGS84 geographical coordinate system.

Satellite-data have very high temporal coverage (more than 99% availability in most of regions). Data for very low sun angles are derived by extrapolation of clear-sky index. The supplied time-series data have all the gaps filled using intelligent algorithms.

Table 3.2: Input data used in the Solargis model

Inputs to Solargis model	Source of input data		Spatial coverage	Time representation	Original time step	Approx. grid resolution
Atmospheric optical depth	MERRA-2 reanalysis	NASA	Global	1994 to 2002	Daily (calculated from 3-hourly)	55 km
	MACC-II reanalysis	ECMWF		2003 to 2012	Daily (calculated from 6-hourly)	125 km
	MACC-II reanalysis			2013 to 2015	Daily (calculated from 3-hourly)	125 km
	MACC-II/CAMS operational			2016 to present	Daily (calculated from 3-hourly)	85 km (since October 2015) 45 km (since June 2016)
Water vapour	CFSR	NOAA	Global	1994 to 2010	1 hour	35 km
	GFS			2011 to 2014	3 hours	55 km
				2015 to present	1 hour	13 km (since February 2015)
Cloud index	Meteosat PRIME	EUMETSAT	Europe and Africa	1994 to 2004	30 minutes	2.5 km at sub-satellite point
				2005 to present	15 minutes	3 km
	Meteosat IODC		South Asia, Middle East, Central Asia, and parts of East Asia	1999 to 2017/02	30 minutes	2.5 km
				2017/03 to present	15 minutes	3 km
	GOES EAST	NOAA	North America and South America	1999 to 2017	30 minutes	4 km
	GOES R			2018 to present	15 minutes*	2 km
	GOES WEST		West North America and Pacific	1999 to 2019/04	30 minutes	4 km
	GOES S			2019/05 to present	10 minutes	2 km
	MTSAT	JMA	East Asia and Western Pacific Rim Countries	2007 to 2015	30 minutes	4 km
	Himawari			2016 to present	10 minutes	2 km
Elevation and horizon	SRTM3	SRTM	Global	-	-	90 and 250 metres

Table 3.3: Approximate pixel size of primary satellite data used for the cloud calculation

Spatial coverage	Satellite area	Nominal Position	Approx. pixel size Lat. 0° (Equator)		Approx. pixel size Lat. 60° North	
			N-S component	E-W component	N-S component	E-W component
Europe, Africa, and parts of Middle East and Brazil	PRIME MFG PRIME MSG	0° 0°	2.5 km 3 km	2.5 km, 3 km	7.3 km 8.8 km	2.7 km 3.3 km
South Asia, Central Asia, and parts of East Asia	IODC MFG IODC MSG	63° E 45° E	2.5 km 3 km	2.5 km 3 km	7.3 km 8.8 km	2.7 km 3.3 km
North America and South America	GOES-EAST GOES R	75° W 75° W	4 km 2 km	4 km 2 km	11.8 km 5.9 km	4.3 km 2.2 km
West North America and Pacific	GOES-WEST GOES S	135° W 135° W	4 km 2 km	4 km 2 km	11.8 km 5.9 km	4.3 km 2.2 km
East Asia and Western Pacific Rim countries	MTSAT Himawari	145° E 145° E	4 km 2 km	4 km 2 km	11.8 km 5.9 km	4.3 km 2.2 km

4 ACCURACY OF SOLARGIS

The accuracy of solar radiation models can be calculated through the **comparison of model outputs** with **ground-data from the reference stations**. The representativeness of such data comparison (satellite and ground-measured) is determined by the precision of the measuring instruments, the maintenance and operational practices, and by quality control of the measured data – in other words, by the measurement accuracy achieved at each measurement station.

The interpretation of these validation statistics and their translation into general and site-specific model uncertainties is discussed in Chapter 5.

4.1 Indicators of model accuracy

The performance of satellite-based models for a given site is characterized by the following indicators, which are calculated for each site for which comparisons with good quality ground measurements are available:

- **Bias or Mean Bias Deviation** (MBD) characterizes systematic model deviation at a given site, i.e. systematic over- or underestimation. Bias values will be above zero when satellite modelled values are overestimating and below zero when underestimating (in comparison to ground measurements).
- **Root Mean Square Deviation** (RMSD) and **Mean Absolute Deviation** (MAD) are used for indicating the spread of deviations for instantaneous values. RMSD indicates discrepancies between short-term modelled values (sub-hourly, hourly, daily, monthly) and ground measurements.

Typically, bias is considered as the first indicator of the model accuracy, however the interpretation of the model accuracy should be done analysing all measures. While knowing bias helps to understand a possible error of the long-term estimate, MAD and RMSD are important for estimating the accuracy of energy simulation and operational calculations (i.e. monitoring and forecasting). Usually validation statistics are normalized and expressed in percentage.

Other indicators can be calculated as well, like **Kolmogorov-Smirnoff Index** (KSI) [1], which characterizes representativeness of distribution of values. It may indicate issues in the model's ability to represent various solar radiation conditions. KSI is important for accurate CSP modelling, as the response of these systems is non-linear to irradiance levels. Even if bias of different satellite-based models is similar, other accuracy characteristics (RMSD, MAD and KSI) may indicate substantial differences in their performance. As the KSI index is dependent on the data sample size, it is used usually for benchmarking of different models or various model versions. As the period of available reference data varies, this index is not used for evaluation of overall model performance.

Besides bias and RMSD, the ability of the model to simulate representatively sub-hourly values for all conditions (especially high and low light conditions) is very important for optimisation of the solar power plants.

4.2 Ground measurements requirements

Only **quality-controlled measurements** from high-quality sensors can be used for objective validation of satellite-based solar model, as issues in the ground measured data would result in a skewed evaluation.

Almost all of the data used in the published validation of Solargis model comply with the requested features described in the table below. Exception are data from RSR instruments used in many validation sites, where uncertainty is in a range from ±4.0 to ±5.0%. In addition, data from several validation sites do not fulfil minimum period criterion – either measurement period was shorter, or some data readings were excluded by data quality control.

Table 4.1: Requirements for ground measured data for being used as model validation reference

Requirement	Description	Comments
High accuracy instruments	"Class A" pyranometers for GHI "Class B" pyrheliometers for DNI	The highest quality and well operated GHI data can have an uncertainty in the range of ±2 to ±3%.
Long enough period measured	At least 12 months of data	In general, the longer period, the better; one year is the minimum for capturing possible seasonal behaviour
Data measured in high temporal resolution	Sub-hourly values Hourly values.	Time stamp adjustments are often required before calculating statistics
Data filtered using quality control procedures applied	Soiling Condensation Misalignment Miscalibration Shadowing Other data issues	Both automated and visual checks are used for identifying incorrect values measured by the ground sensors

4.3 Representativeness of validation sites

Validation statistics for only one site do not provide a representative picture of the model performance in the given geographical conditions. This can be explained by the fact that such site may be affected by a local microclimate or by hidden or residual issues in the ground-measured data.

Therefore, the ability of the model to characterize long-term annual GHI and DNI values should be evaluated at a **sufficient number of validation sites**.

As of today, Solargis model has been validated at 228 public sites worldwide. More than 20 different networks across the globe have been used by Solargis for the validation:

- Global and regional networks: BSRN, SURFRAD, GAW, SOLRAD, ESRL, NREL, FLUXNET, EC, SACC, SRRA, KACST, OPWP, SAURAN, IDMP, Ministry of Energy Chile, etc.
- Data from resource mapping initiatives like ESMAP and IFC (funded by the World Bank Group)
- Meteorological networks of stations at a country level: BOM, KNMI, AEmet, etc.

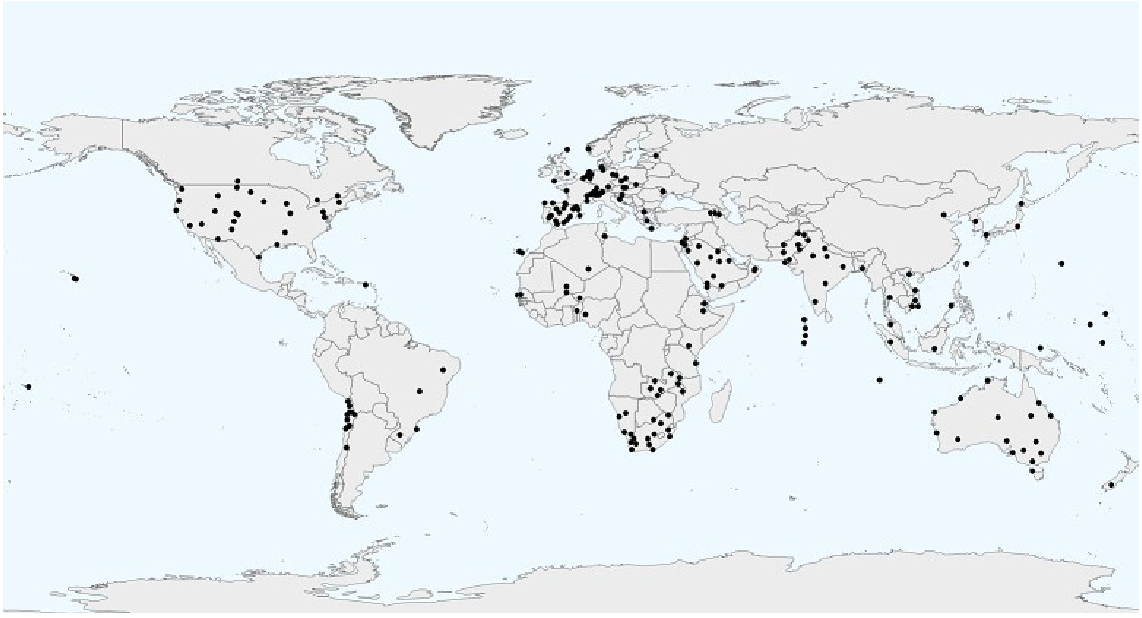

Figure 4.1: Public validation sites used in the validation of Solargis model

Although the number of reference stations is increasing with time, the availability of high-quality ground measurements for comparison is limited for some specific regions. In this case, if a number of validation sites within a specific geography shows bias and RMSD consistently within certain range of values, one can assume that the model will behave consistently also in regions with similar geography where validation sites are not available.

For Solargis, a stable and predictable performance of Solargis is observed across various climate region and bias and RMSD statistics follow a consistent trend. Details are shown in Chapters 4.4 and 4.5.

4.4 Model validation: Bias

After calculating model statistics by comparing Solargis with good quality ground measurements at 228 sites across all type of climates the following has been observed (see Figures 4.2 and 4.3 for map representation and the complete list of sites in Annex).

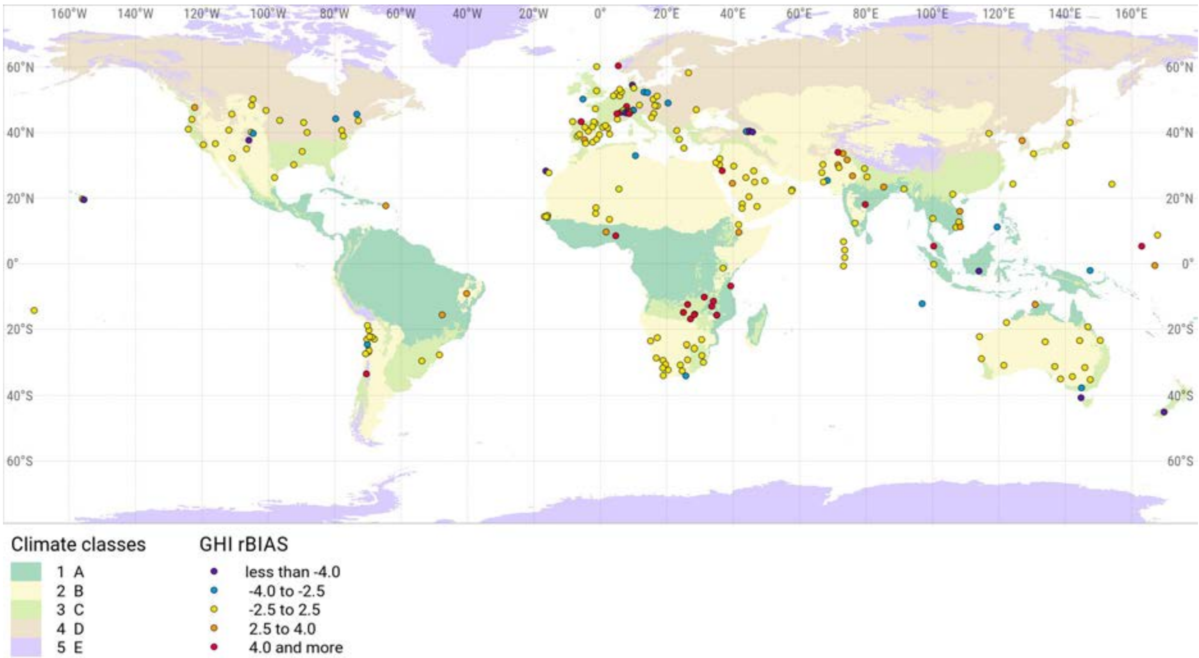

Figure 4.2: Distribution of GHI bias on the background of climate zones (values in percent)
Climatic classes: A – tropical; B – arid; C – temperate; D – cold; E - polar

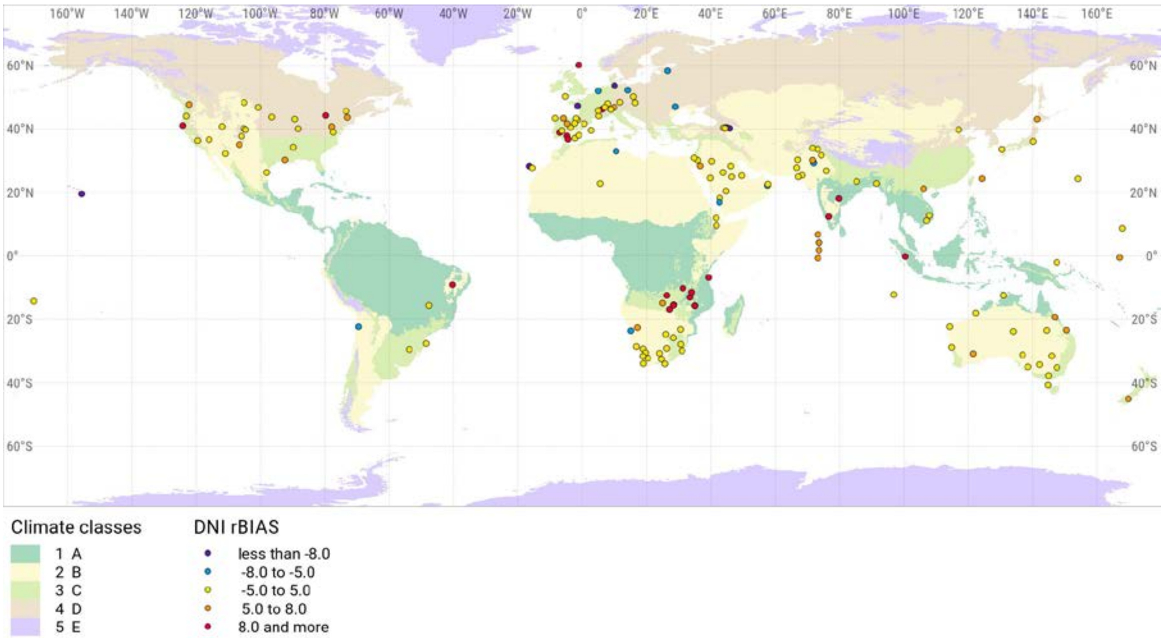

Figure 4.3: Distribution of bias for DNI on the background of climate zones (values in percent)

Even though distribution of validation sites is irregular, a stable and predictable performance of Solargis is observed across various climate regions. The results of the comparison are summarized below. Table 4.2 shows the overall Solargis model performance represented by bias for GHI and DNI parameters for all available validation sites. Tables 4.3 and 4.4 split this information into climate zones.

Table 4.2: Summary of Solargis model accuracy (bias, systematic deviation)

	GHI	DNI	Description
Number of public validation sites	228	166	Sites where data can be open to public access
Mean bias for all sites	0.3%	2.2%	Tendency to overestimate or to underestimate the measured values, on
Standard deviation of biases	±3.0%	±5.3%	Range of deviation of the model estimates assuming normal distribution of bias (68% occurrence)
Occurrence, 80% of sites	±3.9%	±6.8%	Range of deviation of the model estimates assuming normal distribution of bias (80% occurrence)
Occurrence, 90% of sites	±5.0%	±8.7%	Range of deviation of the model estimates assuming normal distribution of bias (90% occurrence)
Occurrence, 98% of sites	±7.0%	±12.3	Range of deviation of the model estimates assuming normal distribution of bias (98% occurrence)
Maximum deviation identified	-8.8% to +12.3%	-15.9% to +18.4%	Maximum model deviation in the set of public validation sites

Table 4.3: Model validation statistics of bias for GHI categorised by climatic zones

	Count	Max [%]	Min [%]	Average [%]	Standard deviation [%]
All climate zones	228	12.3	-8.8	0.3	3.0
Tropical	33	8.6	-4.6	1.7	3.5
Arid	91	5.0	-4.6	-0.1	1.9
Temperate	66	12.3	-8.8	1.5	3.5
Cold	32	6.1	-7.7	-1.1	2.6
Polar	6	1.6	-6.7	-3.0	3.2

Table 4.4: Model validation statistics of bias for DNI categorised by climatic zones

	Count	Max [%]	Min [%]	Average [%]	Standard deviation [%]
All climate zones	166	18.4	-15.9	2.2	5.3
Tropical	23	16.1	-4.6	5.0	5.0
Arid	72	13.8	-7.6	1.0	4.0
Temperate	49	18.4	-10.4	3.7	5.7
Cold	21	9.1	-15.9	0.1	6.3
Polar	1	-8.2	-8.2	-8.2	-

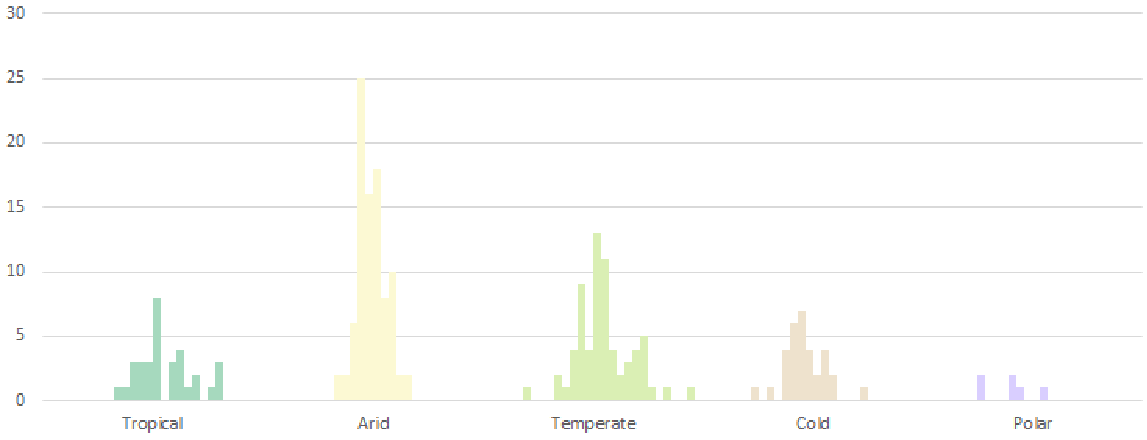

Figure 4.4: Bias distribution of Solargis GHI model outputs by occurrence, categorized by climate

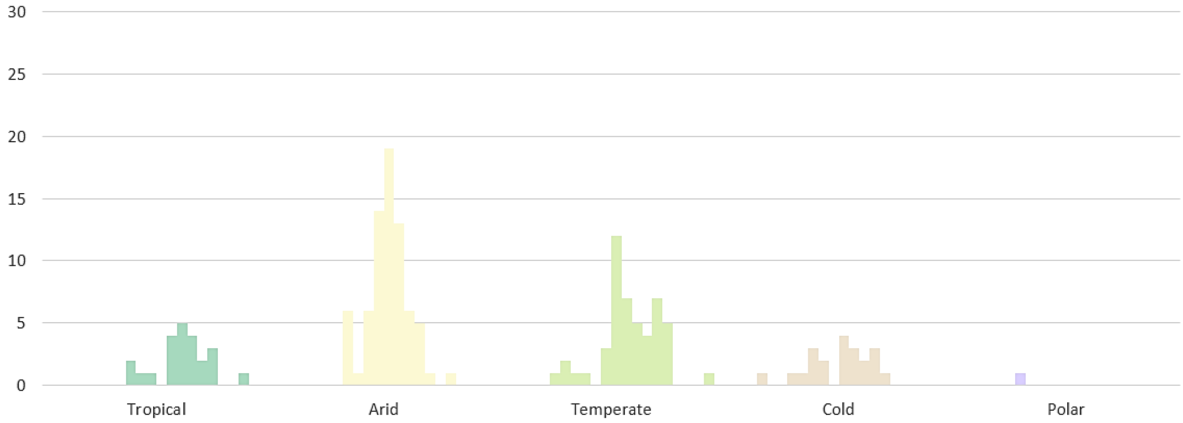

Figure 4.5: Bias distribution of Solargis DNI model outputs by occurrence, categorized by climate

4.5 Model validation: Root mean square deviation

The calculation of Root Mean Square Deviation (RMSD) shows a consistent performance of the model, with a **decreasing value when data is aggregated**. In other words, statistics of hourly values show a higher RMSD in comparison to daily values, and the same happens for daily values in comparison with monthly ones. This is an expected feature from satellite-based models explained by the different nature of data used in the comparison: while the original imagery from the satellite has a maximum spatial resolution of a few kilometres (most variable cloud factor), the measurements from pyranometers and pyrheliometers provide values of a specific point.

Looking at RMSD statistics (Tables 4.5 and 4.6 and Figures 4.6 and 4.7) may provide a first indication of the expected model deviations. However, due to the **variability of deviations expected for different situations**, e.g. for a particular month of the year, or for a particular time during the day, it is difficult to translate these values into particular uncertainties. This would require a more detailed study with longer periods of valid ground data available as a reference.

Table 4.5: Model validation statistics of RMSD for GHI and DNI for all sites

	GHI			DNI		
	RMSD hourly [%]	RMSD daily [%]	RMSD monthly [%]	RMSD hourly [%]	RMSD daily [%]	RMSD monthly [%]
Average value	16.8	8.7	3.8	32.1	19.2	8.0
Standard deviation	6.1	3.6	2.6	11.3	6.8	4.8

Table 4.6: Model validation statistics of RMSD on average, classified by main climatic zones

Climate zone	GHI			DNI		
	RMSD hourly [%]	RMSD daily [%]	RMSD monthly [%]	RMSD hourly [%]	RMSD daily [%]	RMSD monthly [%]
Tropical	20.8	10.0	4.4	39.1	21.0	8.4
Arid	12.2	6.5	2.7	24.7	15.6	6.5
Temperate	18.0	9.1	4.1	35.5	20.5	8.7
Cold	21.1	11.4	4.3	43.9	27.9	11.4
Polar	31.1	18.9	10.5	24.4*	15.2*	8.5*

*Only one site available for this climate zone

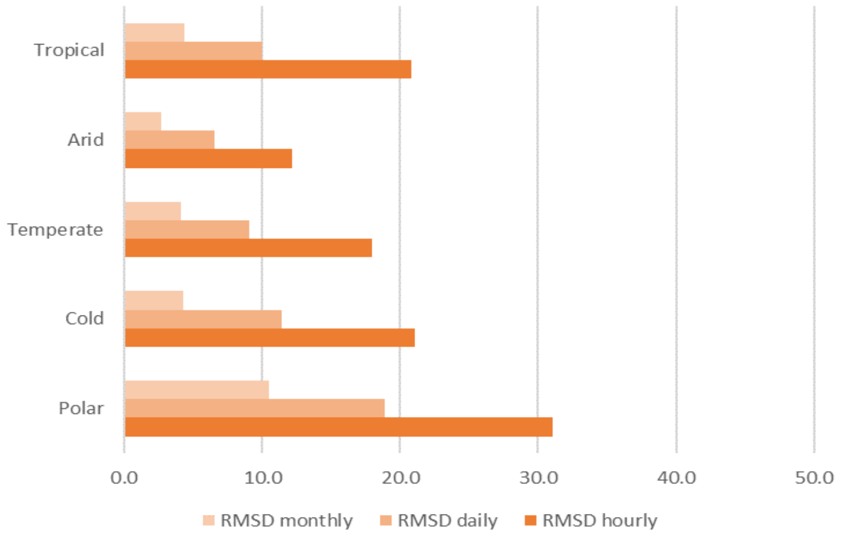

Figure 4.6: Average RMSD of Solargis GHI in % categorized by climate

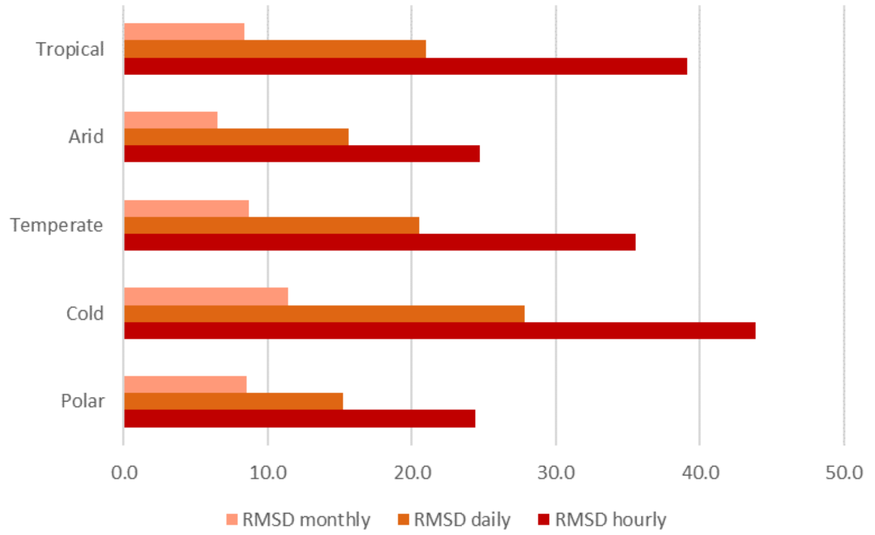

Figure 4.7: Average RMSD of Solargis DNI in % categorized by climate

5 UNCERTAINTY OF SOLAR MODEL: YEARLY ESTIMATES

The accuracy statistics is used for evaluation of the deviation of the site-specific model estimate. The validation statistics, such as bias and RMSD (see Annex) characterize the accuracy of the model in sites where the ground meteorological stations are located.

The validation statistics is affected by local geography and by the quality and reliability of the ground-measured data, which adds an extra difficulty to extrapolate the results to any location outside the validations sites. Provided that the ground-measured data used for the model validation has the required features (see Chapter 4.2), the estimation of Solargis model uncertainty for specific regions and sites can be done at two different levels of detail:

- Simplified estimate, based on the assumption of a normal distribution of identified systematic deviations (Chapters 5.1 to 5.2)
- Advanced estimate based on full analysis of the model uncertainty factors (Chapter 5.3).

5.1 Simplified characterization of bias distribution

The validation statistics for a specific site may not provide representative picture of the model performance in the given geographical conditions. To get better understanding, the model performance should be evaluated from the perspective of validation sites representing similar geographical conditions.

One way of characterizing the possible systematic model deviation (bias) for any location is by accepting a simplified assumption of having a normal distribution of systematic deviations between the model and the measured values. When describing the normal distribution curve, the following facts can be observed:

- **Average of biases is close to zero** (+0.3% for GHI and +2.2% for DNI). This means that there is no systematic tendency either to overestimate or underestimate (distribution is symmetrically centred).
- **Standard deviation of bias is relatively low** (3.0% for GHI and 5.3% for DNI) which is represented by a narrow probability distribution, i.e. the P90 value (value exceeded in the 90% of the cases) will be closer to the P50 (most expected value).

Solargis model is well balanced for both GHI and DNI (and consequently also for DIF), which is demonstrated by the above statistical parameters. As regards the average of biases, even that it is not exactly zero, with high level of confidence, we find the Solargis model well balanced. Forcing the model to show average bias equal to absolute zero would lead to a false belief of perfection, yet in reality it would distort other performance characteristics. The solar model has to be optimised to meet the following four criteria:

1. Minimum systematic error (represented by Bias)
2. Minimum random error (represented by RMSD)
3. Best possible match between high-frequency values (10- or 15- minute values) of the model and the measurements (represented by KSI)
4. Model has to perform in the best possible way in all climate zones and all type of geographies

Any excessive focus on one of the above criteria would lead inevitably to distortion of the performance in some others.

It is also to be reminded that the ground measurements (especially DNI), considered in the model validation as a reference, suffer from imperfections that are inherently present in the data also after rigorous quality control.

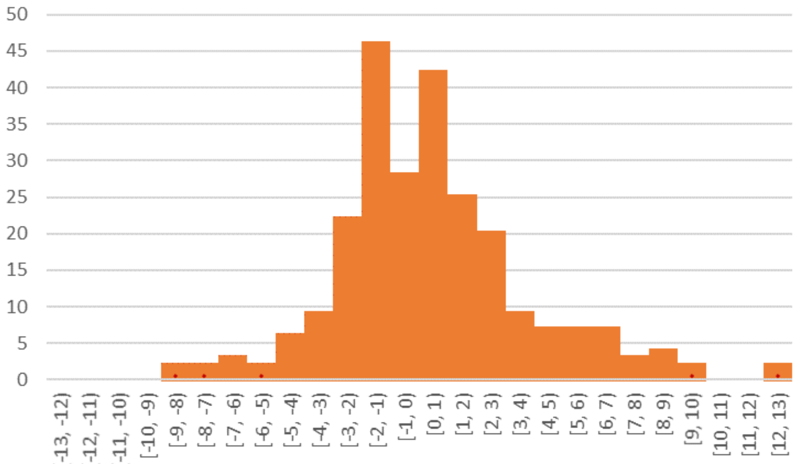

Figure 5.1: GHI bias distribution of the Solargis model

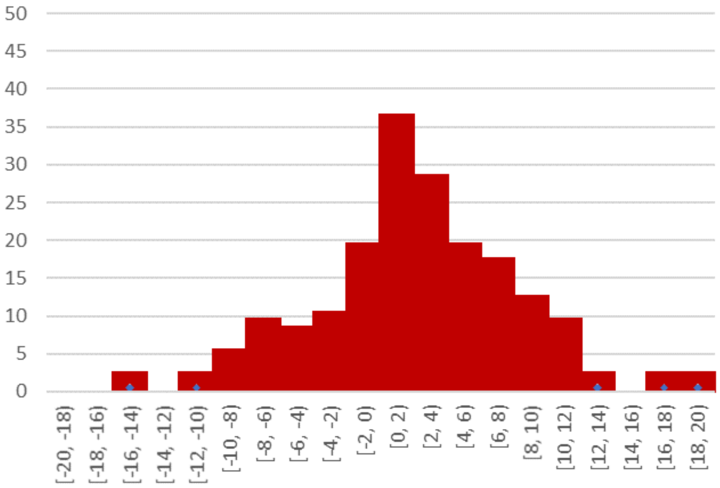

Figure 5.2: DNI bias distribution of the Solargis model

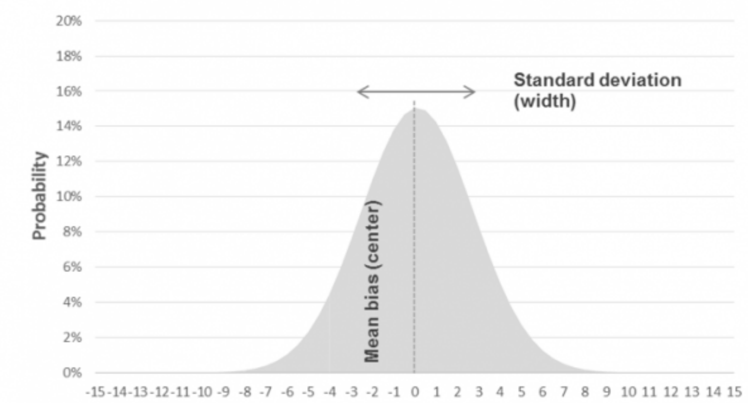

Figure 5.3: Representation of bias probability considering a normal distribution
(Normal distribution is simplified representation of the reality)

If the physics represented by the algorithms is correctly implemented, one can expect robust and uniform behaviour of the model for the geographical conditions, for which it has been calibrated and validated. Yet, as with any other measuring approaches, the user cannot expect zero uncertainty for satellite-based solar models.

The information about the model uncertainty has a probabilistic nature. It generalizes the validation accuracy and it has to be considered at different confidence levels. The expert estimate of the calculation uncertainty in this report (Table 5.1) assumes 80% probability of occurrence of values.

Table 5.1: Estimate of typical Solargis model uncertainty of yearly values

Parameter	Standard deviation of bias values	Expected model uncertainty Occurrence 80% and 98%
Global Horizontal Irradiation (GHI)	3.0%	±4.0 to ±8.0%
Direct Normal Irradiation (DNI)	5.3%	±9.0 to ±14.0%*

* Locally, in specific conditions (e.g. high reflectivity areas), the uncertainty can reach higher values.

5.2 Identification of main situations with low and high uncertainty levels

An analysis on the distribution of the bias across different climate zones and situations lead us to the following conclusions (Figure 7 and Table 5):

- In most situations the expected uncertainty for annual values will be within ±4% for GHI values and ±9% for DNI values:
  - Most of Europe and North America (approx. below 50°N) and Japan.
  - Mediterranean region, Arabian Peninsula (except the Gulf region) and Morocco.
  - South Africa, Chile, Brazil, Australia
- Situations where the expected uncertainty can be as high as ±8% for GHI values and ±14% for DNI values:
  - High latitudes (approx. above 50°)
  - Countries in humid tropical climate (e.g. equatorial regions of Africa, America and Pacific, Philippines, Indonesia and Malaysia) and coastal zones (approx. up to 15 km from a body of water)
  - Regions with high and dynamically changing concentrations of atmospheric aerosols (Northern India, West Africa, Gulf region, some regions in China)
  - High mountains regions with regular snow and ice coverage and high-reflectance deserts
  - Regions with limited or no availability of high-quality ground measurements.

These findings can serve solar model users as a first guidance when analysing the expected uncertainty for a certain site. For estimating a more precise value between these two ranges for a specific location, a more advanced analysis on all factors affecting uncertainty is required (described in the next section).

5.3 Advanced analysis of factors affecting solar model uncertainty

Based on the validation of Solargis data, a location-specific uncertainty estimate can be done after analysing the local climatic and geographic features.

The **accuracy of satellite-based solar and meteorological parameters** depends on the applied numerical models and on the data used as inputs to these models, more specifically, on:

1. Parameterization and adaptation of **numerical models integrated in Solargis** for the given data inputs and their ability to generate accurate results for various geographical and time-variable conditions:
   - Clear-sky model and its capability to properly characterize various states of the atmosphere
   - Simulation accuracy of the satellite model and cloud transmittance algorithms, being able to properly distinguish different types of desert surface, clouds, fog, but also snow and ice.

  - Diffuse and direct decomposition models

2. Accuracy, temporal and spatial resolution of **data inputs for the Solargis model**:
   - Satellite data: their availability, geometric and radiometric corrections, occurrence of artefacts and their mitigation,
   - Parameters describing actual state of the atmosphere, such as aerosols and water vapour,
   - Spatial resolution and accuracy of the Digital Terrain Model (DTM).

To estimate the level of uncertainty for any requested site, the characteristics of the different deviation distributions found, were analysed and confronted with the specific environmental characteristics of each validation site. As a result of this analysis, we identify factors affecting performance of solar model:

- Clouds persistence
- Clouds variability
- Aerosol optical depth
- Total water vapour
- Snow coverage
- Terrain variability
- Distance to water surface
- Anthropogenic pollution
- Satellite pixel distortion
- High albedo surface

This model performance analysis is not an easy task and requires deep and expert knowledge of the model and its internal algorithm and inputs. This needs to be done on a case-by-case basis.

Table 5.2.: Description of the analysis of uncertainty factors for sample locations.

Location	Bratislava Slovakia	Lilongwe Malawi	Maria Elena Chile	Durango Mexico	Detroi t USA	Kurnool India	Canberra Australia
Latitude	48.151°	-13.988	-22.281	24.027	43.338	15.828	-35.280
Longitude	17.109°	33.768	-69.607	-104.653	-83.176	76.311	149.130
Analysis of uncertainty factors							
Clouds persistence	medium	high	no	low	medium	medium	low
Clouds variability	medium	high	low	low	medium	medium	medium
Aerosol optical depth	low	medium	low	medium	medium	high	low
Total water vapour	low	medium	low	low	low	high	low
Snow coverage	medium	no	no	no	medium	no	no
Terrain variability	low	low	low	medium	low	low	low
Distance to water surface	low	low	low	low	medium	low	low
Anthropogenic pollution	low	medium	low	medium	medium	high	low
Satellite pixel distortion	medium	low	low	low	medium	medium	low
High albedo surface	low	low	low	low	low	low	low
Uncertainty estimate (P90)							
GHI uncertainty value	±4.0%	±7.0%	±3.5%	±4.5%	±4.5%	±5.5%	±3.5%
DNI uncertainty value	±9.0%	±13.0%	±9.0%	±11.0%	±9.0%	±13.0%	±8.0%

6 INDEPENDENT VALIDATION STUDIES

Below we show a list of evaluation studies that have been conducted and published by independent organisations. The studies show that Solargis solar model demonstrates robust and harmonized performance.

Satellite or ground-based measurements for production of site-specific hourly irradiance data: Which is most accurate and where? Palmer D., Koubli E., Cole I., Betts T., Gottschalg R., 2018. Solar Energy, 165, 1, 240-255. https://doi.org/10.1016/j.solener.2018.03.029

This research delivers an assessment of which data source is most accurate for production of site specific hourly irradiance data in the UK: satellite-derived values or ground-based measurements. Furthermore, it explores the atmospheric and geographic conditions under which each solar radiation resource delivers the most accurate results. The models tested may be listed in decreasing order of accuracy as follows: Solargis, kriging of ground measurements, CAMS, SARAH and nearest neighbour extrapolation of ground measurements. The exception is where there are at least 6 weather stations per 10,000 km2 grid square. In these circumstances, kriging outperforms Solargis.

Comparison of Annual Global Horizontal Irradiation Maps for Australia. Copper J.K., Bruce A., 2018. Asia Pacific Solar Research Conference, Sydney
https://www.researchgate.net/publication/329642180_Comparison_of_Annual_Global_Horizontal_Irradiation_Maps_for_Australia

This study undertook a cross comparison of the annual global horizontal irradiation data sources available for Australia. The models validated in this study include: Solargis, Meteonorm 7.2, NASA POWER, Vaisala, MERRA- 2, Australian Bureau of Meteorology (BoM) gridded solar data. Besides other conclusions, this study shows that Solargis database demonstrates the lowest bias and RMSD values amongst the compared data sources.

Solar Resource Assessment over Kuwait: Validation of Satellite-derived Data and Reanalysis Modelling. Al-Rasheedi M., Gueymard C.A., Ismail A. and Al-Hajraf S., 2014. EuroSun 2014 Conference Proceedings, 16- 19 September 2014. http://proceedings.ises.org/paper/eurosun2014/eurosun2014-0137-AlRasheedi.pdf

In this, study, ground observations of solar radiation at 5 sites are compared to modeled predictions from various sources. These include a 19-year time series of GHI and DNI obtained from the Solargis satellite model, a 35- year GHI time series from NASA's MERRA reanalysis model, and a 23-year monthly climatology of GHI and DNI from NASA's SSE database. The long-term monthly mean GHI values obtained from MERRA and site-adapted Solargis show reasonable agreement. GHI from the raw Solargis and the SSE GHI data, as well as most predictions of DNI, exhibit significant differences, likely because of diverging estimates of aerosol effects. The Solargis time series is significantly improved by its site adaptation. When derived from either MERRA or Solargis, both the GHI inter-annual variability and its long-term trend disagree substantially, which requires additional scrutiny

Long Term Satellite Global, Beam and Diffuse Irradiance Validation. Ineichen P., 2014. Energy Procedia, 48, 1586-1596. https://doi.org/10.1016/j.egypro.2014.02.179.

This study presents results of a validation in the European and Mediterranean region of satellite-derived irradiation databases in hourly, daily and monthly values. GHI and DNI data from 6 satellite-irradiance-models were compared with high quality measurements from 18 locations. Up to 16 years of continuous measurements have been used for the validation. The locations chosen for validation cover different climate conditions - from desert to oceanic, and the altitudes from sea level to 1580 metres. Solargis was identified as the data source with the lowest overall bias, lowest mean bias deviation, and lowest RMSD.

Long term satellite hourly, daily and monthly global, beam and diffuse irradiance validation. Interannual variability analysis. Ineichen P., 2013. University of Geneva/IEA SHC Task 46, 2013.
http://solargis.com/support/accuracy-and-comparisons/independent-comparisons/

Five different satellite products deriving both global and beam irradiance are validated against data from 23 ground sites.

7 CONCLUSIONS

Solargis solar radiation model is based on the best available and scientifically proven scientific models, all of them adapted to the modern input data sources and methods and implemented into a processing chain by team Solargis. The model is designed to perform in a balanced way (low bias, RMSD and KSI) in all geographical conditions. The model has been validated using approx. 1000 validation sites where solar and atmospheric (aerosols) measurements are available. Out of this, a subset of 228 public sites was used for preparing this technical report.

Over the operation period of almost 10 years the model is being constantly improved and validated on thousands utility scale and large-scale projects being constructed in almost 100 countries. The quality and reliability of the model is one of reasons, why its outputs have been used by about 900 small to large companies worldwide in year 2019. The model is supported by continuous research and development resulting in a large number of peer-reviewed papers in the scientific journals.

We are committed to continuous development and implementation of new data sets and methodologies. The roadmap of our research includes works on new solar models and data delivery approaches, some of them will be included in the production in year 2020. The research also includes delivery of added-value data products, such as Typical Meteorological Year data for various probabilities of occurrence, site adapted time series, 1-minute data generator.

The historical and real-time updated time series and added-value data products are accessible through Solargis online services, automatic and interactive for almost any land surface in the world.

8 ACRONYMS

AERONET	The AERONET (AErosol RObotic NETwork) is a ground-based remote sensing network dedicated to measure atmospheric aerosol properties. It provides a long-term database of aerosol optical, microphysical and radiative parameters.
AOD	Aerosol Optical Depth at 670 nm. This is one of atmospheric parameters derived from MACC database and used in Solargis. It has important impact on accuracy of solar calculations in arid zones.
CFSR	Climate Forecast System Reanalysis. The meteorological model operated by the US service NOAA.
CPV	Concentrated Photovoltaic systems, which uses optics such as lenses or curved mirrors to concentrate a large amount of sunlight onto a small area of photovoltaic cells to generate electricity.
CSP	Concentrated solar power systems, which use mirrors or lenses to concentrate a large amount of sunlight onto a small area, where it is converted to heat for a heat engine connected to an electrical power generator.
DIF	Diffuse Horizontal Irradiation, if integrated solar energy is assumed. Diffuse Horizontal Irradiance, if solar power values are discussed.
DNI	Direct Normal Irradiation, if integrated solar energy is assumed. Direct Normal Irradiance, if solar power values are discussed.
ECMWF	European Centre for Medium-Range Weather Forecasts is independent intergovernmental organisation supported by 34 states, which provide operational medium- and extended-range forecasts and a computing facility for scientific research.
EUMETSAT	European Organisation for the Exploitation of Meteorological Satellites
Himawari 8	Geostationary weather satellite operated by the Japanese Meteorological Agency (JMA), operational since the year 2017
GFS	Global Forecast System. The meteorological model operated by the US service NOAA.
GHI	Global Horizontal Irradiation, if integrated solar energy is assumed. Global Horizontal Irradiance, if solar power values are discussed.
GOES	Geostationary Operational Environmental Satellite (NOAA NESDIS)
GTI	Global Tilted (in-plane) Irradiation, if integrated solar energy is assumed. Global Tilted Irradiance, if solar power values are discussed.
MACC	Monitoring Atmospheric Composition and Climate – meteorological model operated by the European service ECMWF (European Centre for Medium-Range Weather Forecasts)
MERRA-2	Modern Era Reanalysis for Research and Applications, service operated by NASA
Meteosat MFG	Meteosat satellite operated by EUMETSAT organization. MFG: Meteosat First Generation.
Meteosat MSG	Meteosat satellite operated by EUMETSAT organization. MSG: Meteosat Second Generation.
MTSAT 2	Multifunctional Transport Satellite operated by Japan Meteorological Agency (JMA), also known as Himawari 7, positioned at 145° East
NOAA	National Oceanic and Atmospheric Administration

NCEP	National Centre for Environmental Prediction
PVOUT	Photovoltaic electricity output often presented as percentage of installed DC power of the photovoltaic modules. This unit is calculated as a ratio between output power of the PV system and the cumulative nominal power at the label of the PV modules (Power at Standard Test Conditions).
SRTM	Shuttle Radar Topography Mission
TEMP	Air Temperature at 2 metres
WRF	Weather Research and Forecasting model

9 GLOSSARY

Aerosols	Small solid or liquid particles suspended in air, for example clouds, haze, and air pollution such as smog or smoke.
All-sky irradiance	The amount of solar radiation reaching the Earth's surface is mainly determined by Earth-Sun geometry (the position of a point on the Earth's surface relative to the Sun which is determined by latitude, the time of year and the time of day) and the atmospheric conditions (the level of cloud cover and the optical transparency of atmosphere). All-sky irradiance is computed with all factors taken into account
Bias	Represents systematic deviation (over- or underestimation) and it is determined by systematic or seasonal issues in cloud identification algorithms, coarse resolution and regional imperfections of atmospheric data (aerosols, water vapour), terrain, sun position, satellite viewing angle, microclimate effects, high mountains, etc. Bias values will be positive when satellite modelled values are overestimating and negative when underestimating (in comparison to ground measurements). $Bias = X^{k}{}_{modeled} - X^{k}_{measured}$
Clear-sky irradiance	The clear sky irradiance is calculated similarly to all-sky irradiance but without taking into account the impact of cloud cover.
Frequency of data (10/15/30 minute, hourly, daily, monthly, yearly)	Period of aggregation of solar data that can be obtained from the Solargis database.
Long-term average	Average value of selected parameter (GHI, DNI, etc.) based on multiyear historical time series. Long-term averages provide a basic overview of solar resource availability and its seasonal variability. Alternative terminology: long-term prediction, long-term forecasts.
Root Mean Square Deviation (RMSD)	Represents spread of deviations given by random discrepancies between measured and modelled data and is calculated according to this formula: $RMSD = \sqrt{\frac{\sum_{k=1}^{n}\left(X^{k}{}_{measured} - X^{k}_{modeled}\right)^{2}}{n}}$ On the modelling side, this could be low accuracy of cloud estimate (e.g. intermediate clouds), under/over estimation of atmospheric input data, terrain, microclimate and other effects, which are not captured by the model. Part of this discrepancy is natural - as satellite monitors large area (of approx. 3 x 4 km), while sensor sees only micro area of approx. 1 sq. centimetre. On the measurement side, the discrepancy may be determined by accuracy/quality and errors of the instrument, pollution of the detector, misalignment, data loggers, insufficient quality control, etc. Alternative terminology: Root Mean Square Error (RMSE)
Site adaptation	Application of accuracy-enhancement methods that are capable to adapt satellite-derived DNI and GHI datasets (and derived parameters) to the local climate conditions that cannot be recorded in the original satellite and atmospheric inputs. The data adaptation is important especially when specific situations such as extreme irradiance events are important to be correctly represented in the enhanced dataset. However, the methods have to be used carefully, as inappropriate use for non-systematic deviations or use of less accurate ground data leads to accuracy degradation of the primary satellite-derived dataset. Alternative term: correlation, calibration.
Solar irradiance	Solar power (instantaneous energy) falling on a unit area per unit time [W/m^2]. Solar resource or solar radiation is used when considering both irradiance and irradiation.

Solar irradiation	Amount of solar energy falling on a unit area over a stated time interval [Wh/m^2 or kWh/m^2].
Solar radiation	The term embraces both solar irradiance and solar irradiation terms. Solar radiation, selectively attenuated by the atmosphere, which is not reflected or scattered and reaches the surface directly, is beam (direct) radiation. The scattered radiation that reaches the ground is diffuse radiation. The small part of radiation that is reflected from the ground onto the inclined receiver is reflected radiation. These three components of radiation together create global radiation.
Spatial grid resolution	In digital cartography the term applies to the minimum size of the grid cell or in the other words minimal size of the pixels in the digital map
Uncertainty	Is a parameter characterizing the possible dispersion of the values attributed to an estimated irradiance/irradiation values. The best estimate or median value is also called P50 value. For annual and monthly solar irradiation summaries it is close to average, since multiyear distribution of solar radiation resembles closely normal distribution. Uncertainty assessment of the solar resource estimate is based on a detailed understanding of the achievable accuracy of the solar radiation model and its data inputs (satellite, atmospheric and other data), which is confronted by an extensive data validation experience. The second important source of uncertainty information is the understanding of quality issues of ground measuring instruments and methods, as well as the methods correlating the ground-measured and satellite-based data. For instance, the range of uncertainty may assume 80% probability of *occurrence* of values, so the lower boundary (negative value) of uncertainty represents 90% probability of *exceedance*, and it is also used for calculating the P90 value (normal distribution is assumed). Similarly, other confidence intervals can be considered (P75, P95, P99 values, etc.)
Water vapour	Water in the gaseous state. Atmospheric water vapour is the absolute amount of water dissolved in air.

10 LIST OF FIGURES

Figure 3.1: Historical data availability 8

Figure 3.2: Global Horizontal Irradiation: Long term yearly average or daily/yearly summaries........ 9

Figure 3.3: Direct Normal Irradiation: Long term yearly average or daily/yearly summaries 9

Figure 3.4: Scheme of the semi-empirical solar radiation model (Solargis)........10

Figure 3.5: Satellite missions used for cloud identification 11

Figure 4.1: Public validation sites used in the validation of Solargis model 15

Figure 4.2: Distribution of GHI bias on the background of climate zones (values ion percent)........16

Figure 4.3: Distribution of bias for DNI on the background of climate zones (values in percent) 17

Figure 4.4: Bias distribution of Solargis GHI model outputs by occurrence, categorized by climate 18

Figure 4.5: Bias distribution of Solargis DNI model outputs by occurrence, categorized by climate 19

Figure 4.6: Average RMSD of Solargis GHI in % categorized by climate 20

Figure 4.7: Average RMSD of Solargis DNI in % categorized by climate........20

Figure 5.1: GHI bias distribution of the Solargis model 22

Figure 5.2: DNI bias distribution of the Solargis model........ 22

Figure 5.3: Representation of bias probability considering a normal distribution 22

11 LIST OF TABLES

Table 2.1: Solar resource parameters provided by Solargis to solar power industry..5
Table 2.2: Comparing solar measurements and model data...6
Table 3.1: Solargis solar resource data: Summary of technical features 8
Table 3.2: Input data used in the Solargis model 12
Table 3.3: Approximate pixel size of primary satellite data used for the cloud calculation 13
Table 4.1: Requirements for ground measured data for being used as model validation reference 15
Table 4.2: Summary of Solargis model accuracy (bias, systematic deviation) 17
Table 4.3: Model validation statistics of bias for GHI categorised by climatic zones 18
Table 4.4: Model validation statistics of bias for DNI categorised by climatic zones 18
Table 4.5: Model validation statistics of RMSD for GHI and DNI for all sites... 19
Table 4.6: Model validation statistics of RMSD on average, classified by main climatic zones.................................. 19
Table 5.1: Estimate of typical Solargis model uncertainty of yearly values.. 23
Table 5.2.: Description of the analysis of uncertainty factors for sample locations 24

12 REFERENCES

[1] Espinar B., Ramírez L., Drews A., Beyer H. G., Zarzalejo L. F., Polo J., Martín L., Analysis of different comparison parameters applied to solar radiation data from satellite and German radiometric stations. Solar Energy, 83, 1, 118-125, 2009.

[2] Perez R., Cebecauer T., Šúri M., 2013. Semi-Empirical Satellite Models. In Kleissl J. (ed.) Solar Energy Forecasting and Resource Assessment. Academic press. http://www.sciencedirect.com/science/article/pii/B9780123971777000024

[3] Cebecauer T., Šúri M., Perez R., High performance MSG satellite model for operational solar energy applications. ASES National Solar Conference, Phoenix, USA, 2010. http://solargis.com/assets/publication/2010/Cebecauer-Suri-Perez--ASES2010--High-performance-MSG-satellite-model-for-operational-solar-energy-applications.pdf

[4] Šúri M., Cebecauer T., Perez P., 2010. Quality Procedures of Solargis for Provision Site-Specific Solar Resource Information. Conference SolarPACES 2010, September 2010, Perpignan, France. http://solargis.com/assets/publication/2010//Suri-Cebecaue--Perez-SolarPACES2010--Quality-procedures-of-solargis-for-provision-site-specific-solar-resource-information.pdf

[5] Ineichen P., A broadband simplified version of the Solis clear sky model, 2008. Solar Energy, 82, 8, 758-762.

[6] Morcrette J., Boucher O., Jones L., Salmond D., Bechtold P., Beljaars A., Benedetti A., Bonet A., Kaiser J.W., Razinger M., Schulz M., Serrar S., Simmons A.J., Sofiev M., Suttie M., Tompkins A., Uncht A., GEMS- AER team, 2009. Aerosol analysis and forecast in the ECMWF Integrated Forecast System. Part I: Forward modelling. Journal of Geophysical Research, 114.

[7] Benedictow A. et al. 2012. Validation report of the MACC reanalysis of global atmospheric composition: Period 2003-2010, MACC-II Deliverable D83.1.

[8] Molod, A., Takacs, L., Suarez, M., and Bacmeister, J., 2015: Development of the GEOS-5 atmospheric general circulation model: evolution from MERRA to MERRA2, Geosci. Model Dev., 8, 1339-1356, doi:10.5194/gmd-8-1339-2015

[9] Cebecauer T., Šúri M., Accuracy improvements of satellite-derived solar resource based on GEMS re-analysis aerosols. Conference SolarPACES 2010, September 2010, Perpignan, France. http://solargis.com/assets/publication/2010/Cebecauer-Suri--SolarPACES2010--Accuracy-improvements-of- satellite-derived-solar-resource-based-on-GEMS-re-analysis-aerosols.pdf

[10] Cebecauer T., Perez R., Šúri M., Comparing performance of Solargis and SUNY satellite models using monthly and daily aerosol data. Proceedings of the ISES Solar World Congress 2011, September 2011, Kassel, Germany. http://solargis.com/assets/publication/2011/Cebecauer-Perez-Suri--ISES2011--Comparing-performance-of-Solargis-and-SUNY-satellite-models-using-monthly-and-daily-aerosol-data.pdf

[11] GFS model. http://www.nco.ncep.noaa.gov/pmb/products/gfs/

[12] CFSR model. https://climatedataguide.ucar.edu/climate-data/climate-forecast-system-reanalysis-cfsr/

[13] CFSv2 model http://www.cpc.ncep.noaa.gov/products/CFSv2/CFSv2seasonal.shtml

[14] Cano D., Monget J.M., Albuisson M., Guillard H., Regas N., Wald L., 1986. A method for the determination of the global solar radiation from meteorological satellite data. Solar Energy, 37, 1, 31–39.

[15] Perez R., Ineichen P., Maxwell E., Seals R. and Zelenka A., 1992. Dynamic global-to-direct irradiance conversion models. ASHRAE Transactions-Research Series, pp.354-369.

[16] Perez, R., Seals R., Ineichen P., Stewart R., Menicucci D., 1987. A new simplified version of the Perez diffuse irradiance model for tilted surfaces. Solar Energy, 39,221-232.

[17] Ruiz-Arias J.A., Cebecauer T., Tovar-Pescador J., Šúri M., 2010. Spatial disaggregation of satellite-derived irradiance using a high-resolution digital elevation model. Solar Energy, 84,1644-57. http://www.sciencedirect.com/science/article/pii/S0038092X10002136

[18] Ineichen P. Long term satellite hourly, daily and monthly global, beam and diffuse irradiance validation. Interannual variability analysis. University of Geneva/IEA SHC Task 46, 2013. http://solargis.com/support/accuracy-and-comparisons/independent-comparisons/

[19] Copper J.K., and Bruce A., 2018. Comparison of Annual Global Horizontal Irradiation Maps for Australia. University of New South Wales. https://www.researchgate.net/publication/329642180_Comparison_of_Annual_Global_Horizontal_Irradiatio

n_Maps_for_Australia

[20] Al-Rasheedi M., Gueymard C.A., Ismail A. and Al-Hajraf S., 2014. Solar Resource Assessment over Kuwait: Validation of Satellite-derived Data and Reanalysis Modeling, EuroSun 2014 Conference Proceedings, 16- 19 September 2014. http://proceedings.ises.org/paper/eurosun2014/eurosun2014-0137-AlRasheedi.pdf

[21] Palmer D., Koubli E., Cole I., Betts T., Gottschalg R., 2018. Satellite or ground-based measurements for production of site-specific hourly irradiance data: Which is most accurate and where? Solar Energy, 165, 1, 240- 255. https://doi.org/10.1016/j.solener.2018.03.029

13 SUPPORT INFORMATION

13.1 Background on Solargis

Solargis is a technology company offering energy-related meteorological data, software and consultancy services to solar energy. We support industry in the site qualification, planning, financing and operation of solar energy systems for more than 19 years. We develop and operate a new generation high-resolution global database and applications integrated within Solargis® information system. Accurate, standardised and validated data help to reduce the weather-related risks and costs in system planning, performance assessment, forecasting and management of distributed solar power.

13.2 Legal information

Considering the nature of climate fluctuations, interannual and long-term changes, as well as the uncertainty of measurements and calculations, company Solargis cannot take guarantee of the accuracy of estimates. Company Solargis has done maximum possible for the assessment of climate conditions based on the best available data, software and knowledge. Solargis**®** is the registered trademark of company Solargis. Other brand names and trademarks that may appear in this study are the ownership of their respective owners.

ISO 9001
LL-C (Certification)

Solargis is ISO 9001:2015 certified company for quality management.

[22]

14 ANNEX

List of validation sites

Site name	Country	GHI	DNI	Latitude [°]	Longitude [°]	Elevation [m a.s.l.]	Source	Climate zone	Recently updated
A Coruna	Spain	x	x	43.3672	-8.4194	58	AEMET	3	No
Abha	Saudi Arabia	x	x	18.2300	42.6600	2039	KACST	2	No
Adam	Oman	x	x	22.2072	57.5230	250	OPWP	2	Yes
Adelaide	Australia	x	x	-34.9524	138.5204	2	BoM	2	Yes
Aggeneys	South Africa	x	x	-29.2945	18.8155	789	Eskom	2	Yes
Agoufu	Mali	x	-	15.3445	-1.4791	290	-	2	Yes
Al-Ahsa	Saudi Arabia	x	x	25.3000	49.4800	178	KACST	2	No
Al-Jouf	Saudi Arabia	x	x	29.7900	40.1000	669	KACST	2	No
Al-Madinah	Saudi Arabia	x	x	24.5500	39.7000	626	KACST	2	No
Al-Qaisumah	Saudi Arabia	x	x	28.3200	46.1300	358	KACST	2	No
Alamosa	Colorado, USA	x	x	37.6969	-105.9232	2317	SURFRAD	2	Yes
Albuquerque	New Mexico, USA	x	x	35.0380	-106.6221	1617	NOAA ISIS	2	Yes
Alice Springs	Australia	x	x	-23.7951	133.8890	546	BoM	2	Yes
Almeria PSA	Spain	x	x	37.0928	-2.3624	560	PSA, DLR	2	Yes
American Samoa Observatory	ASM	x	x	-14.2474	-170.5644	42	NOAA ESRL	1	No
Amman	Jordan	x	-	32.0247	35.8789	1041	-	3	No
Armazones	Chile	x	-	-24.6346	-70.2426	2576	Ministerio de energia	2	Yes
Athens	Greece	x	-	37.9718	23.7183	107	IDMP	3	Yes
BacNinh	Vietnam	x	x	21.2015	106.0629	60	ESMAP	3	Yes
Badajoz	Spain	x	x	38.8861	-7.0117	175	AEMET	3	No
Bahawalpur	Pakistan	x	x	29.3254	71.8188	123	ESMAP	2	Yes
Bamba	Mali	x	-	17.0990	-1.4018	272	-	2	Yes
Banizoumbou	Niger	x	-	13.5311	2.6613	211	-	2	Yes
Barcelona	Spain	x	-	41.3858	2.1169	125	SOLARFLUX	3	No
Bergen	Norway	x	-	60.3838	5.3319	45	IDMP Univ. of Bergen	3	Yes
Bismarck	North Dakota, USA	x	x	46.7718	-100.7596	503	NOAA ISIS	4	Yes
Bloemfontein	South Africa	x	x	-29.1107	26.1850	1432	SAURAN	2	No
Bondville	Illinois, USA	x	x	40.0519	-88.3731	230	SURFRAD	4	Yes
Boulder	Colorado, USA	x	x	40.1250	-105.2368	1689	SURFRAD	2	Yes

Site name	Country	GHI	DNI	Latitude [°]	Longitude [°]	Elevation [m a.s.l.]	Source	Climate zone	Recently updated
Bovoni 2, St. Thomas	Virgin Islands, USA	x	-	17.7080	-64.6933	28	NREL	1	Yes
Bozeman	Montana, USA	x	-	45.6620	-111.0450	1507	SOLRADNET	4	Yes
Brasilia	Brasil	x	x	-15.6010	-47.7130	1023	BSRN	1	Yes
Bratislava	Slovakia	x	-	48.1695	17.0715	195	IDMP	4	No
Broome	Australia	x	x	-17.9475	122.2353	7	BoM	2	Yes
Bukit Kototabang	Indonesia	x	x	-0.2019	100.3181	864	GAW	1	No
Cabauw	Netherlands	x	-	51.9667	4.9167	0	KNMI	3	No
Caceres	Spain	x	x	39.4722	-6.3394	405	AEMET	2	No
Camborne	UK	x	x	50.2167	-5.3167	88	BSRN	3	No
Cape Grim	Australia	x	x	-40.6817	144.6892	95	BoM	3	Yes
Carpentras	France	x	x	44.0830	5.0590	100	BSRN	3	Yes
Cener	Spain	x	x	42.8160	-1.6010	471	BSRN	3	Yes
Central Highlands	Vietnam	x	x	12.7534	107.8763	290	ESMAP	1	Yes
Cerro Calan de	Chile	x	-	-33.3973	-70.5368	795	ministerio energia	3	Yes
Chilanga	Malawi	x	x	-15.6798	34.9723	767	ESMAP	1	Yes
Chileka	Malawi	x	x	-15.6798	34.9723	767	ESMAP	1	Yes
Cimetta	Switzerland	x	-	46.2011	8.7899	1670	-	4	No
Cobar	Australia	x	x	-31.4840	145.8294	260	BOM	2	Yes
Copiapo	Chile	x	-	-27.2646	-70.7806	203	Ministerio de energia	2	Yes
Cordoba	Spain	x	x	37.8444	-4.8506	91	AEMET	3	No
Crete_TEI	Greece	x	-	35.2997	25.1000	122	SOLARFLUX	3	No
Crucero2	Chile	x	x	-22.2745	-69.5663	1185	Ministerio de energia	2	Yes
DaNang	Vietnam	x	-	16.0126	108.1865	24	ESMAP	1	Yes
Dar es Salaam	Tanzania	x	x	-6.7811	39.2039	93	ESMAP	1	Yes
Darwin	Australia	x	x	-12.4239	130.8925	30	BoM	1	Yes
Davos	Switzerland	x	-	46.8132	9.8445	1586	-	4	No
De Aar	South Africa	x	x	-	24.0000	1331	BSRN	2	No
Desert Rock	Nevada, USA	x	x	36.6237	-116.0195	1007	SURFRAD	2	Yes
Dicheto	Ethiopia	x	x	11.9156	41.5511	431	IFC	2	Yes
Djougou	Benin	x	-	9.6920	1.6620	438	-	1	Yes
Durban 1	South Africa	x	x	-29.8710	30.9769	136	SAURAN	3	No
Edinburg	Texas, USA	x	x	26.3059	-98.1716	45	NREL	2	Yes
Egbert	Canada	x	x	44.2300	-79.7800	233	SACC	4	Yes
Eggishorn	Switzerland	x	-	46.4273	8.0927	2895	-	5	No
El Nido Airport	Philippines	x	-	11.2050	119.4130	4	SOLARFLUX	1	No

Site name	Country	GHI	DNI	Latitude [°]	Longitude [°]	Elevation [m a.s.l.]	Source	Climate zone	Recently updated
El Saler	Spain	x	-	39.3460	-0.3190	10	In. 2011 (FluxNet)	2	No
Ell	Netherlands	x	-	51.2000	5.7667	30	KNMI	3	No
Eugene	Oregon, USA	x	x	44.0467	-123.0743	134	NREL	3	Yes
Fatick	Senegal	x	-	14.3675	-16.4135	8	IFC	2	Yes
Feni	Bangladesh	x	x	22.8003	91.3582	15	ESMAP	1	Yes
Florianopolis	Brasil	x	x	-27.6047	-48.5227	11	BSRN	3	Yes
Fort Peck	Montana, USA	x	x	48.3078	-105.1017	634	SURFRAD	2	Yes
Freiburg	Germany	x	x	47.9792	7.8311	275	IDMP	3	No
Fukuoka	Japan	x	x	33.5817	130.3750	3	BSRN	3	Yes
Gaborone	Botswana	x	x	-24.6619	25.9318	977	SAURAN	2	Yes
Gan	Maldives	x	x	-0.6906	73.1501	2	ESMAP	1	Yes
Ganovce	Slovakia	x	-	49.0333	20.3167	706	GAW	4	No
Geneve	Switzerland	x	x	46.2003	6.1316	420	CUEPE	3	No
Geraldton	Australia	x	x	-28.8047	114.6980	30	BoM	3	Yes
Gizan	Saudi Arabia	x	x	16.9000	42.5800	7	KACST	2	No
Gobabeb	Namibia	x	x	-23.5614	15.0420	407	BSRN	2	Yes
Goodwin Creek	Mississippi, USA	x	x	34.2547	-89.8729	98	SURFRAD	3	Yes
Gornergrat	Switzerland	x	-	45.9842	7.7851	3110	-	5	No
Gospic	Croatia	x	-	44.5486	15.3613	565	-	4	No
Graaff-Reinet	South Africa	x	x	-32.4855	24.5858	660	SAURAN	2	No
Hamburg	Germany	x	-	53.6333	10.0000	14	-	3	No
Hanford	California, USA	x	x	36.3136	-119.6316	73	NOAA ISIS	2	Yes
Hanimaadhoo	Maldives	x	x	6.7464	73.1686	2	ESMAP	1	Yes
Heino	Netherlands	x	-	52.4333	6.2667	4	KNMI	3	No
Helios	South Africa	x	x	-30.5011	19.5607	905	Eskom	2	Yes
Hradec Kralove	Czech republic	x	x	50.1830	15.8330	236	CHMU	4	No
Hrazdan	Armenia	x	x	40.5116	44.8230	1845	ESMAP	4	Yes
Hulhulé	Maldives	x	x	4.1927	73.5281	2	ESMAP	1	Yes
Hurso	Ethiopia	x	x	9.6136	41.6385	1110	IFC	2	Yes
Hyderabad	Pakistan	x	x	25.4134	68.2595	63	ESMAP	2	Yes
Ilorin	Nigeria	x	-	8.5333	4.5667	273	BSRN	1	No
Inca de Oro	Chile	x	-	-26.7532	-69.9060	1580	ministerio de energia	2	Yes
Ishigakijima	Japan	x	x	24.3367	124.1633	11	BSRN	1	Yes
Islamabad	Pakistan	x	x	33.6419	72.9838	558	ESMAP	3	Yes
Ispra	Italy	x	-	45.8120	8.6271	220	-	3	No
Izana	Canary Isl.	x	x	28.3089	-16.4994	2371	BSRN	3	No

Site name	Country	GHI	DNI	Latitude [°]	Longitude [°]	Elevation [m a.s.l.]	Source	Climate zone	Recently updated
Jaipur	India	x	-	26.8090	75.8620	403	SRRA	2	Yes
Jungfraujoch	Germany	x	-	46.5488	7.9850	3580	-	5	No
Kadhdhoo	Maldives	x	x	1.8583	73.5197	2	ESMAP	1	Yes
Kahone	Senegal	x	-	14.1686	-16.0342	10	IFC	2	Yes
Kailua-Kona	Hawaii, USA	x	-	19.7275	-156.0590	4	NREL	1	No
Kalgoorlie-Boulder	Australia	x	x	-30.7847	121.4533	365	BOM	2	Yes
Kanpur	India	x	-	26.5127	80.2319	123	SolRadNet	3	No
Karachi	Pakistan	x	x	24.9334	67.1116	45	ESMAP	2	Yes
Kasungu	Malawi	x	x	-13.0153	33.4685	1065	ESMAP	3	Yes
Keeling	Cocos Islands	x	x	-12.1892	96.8344	3	BSRN	1	Yes
Khuzdar	Pakistan	x	x	27.8178	66.6294	1254	ESMAP	2	Yes
Kishinev	Moldova	x	x	47.0013	28.8156	205	BSRN	4	No
Kosrae	Micronesia	x	-	5.3529	162.9570	0	-	1	Yes
Kwajalein	Micronesia	x	x	8.7200	167.7310	10	BSRN	1	Yes
Lafayette	Louisiana, USA	x	x	30.2050	-92.3979	5	NREL	3	Yes
Lahore	Pakistan	x	x	31.6946	74.2441	207	ESMAP	2	Yes
Lauder	New Zealand	x	x	-	169.6890	350	BSRN	2	Yes
Learmonth	Australia	x	x	-22.2406	114.0970	5	BoM	2	Yes
Leeuwarden	Netherlands	x	-	53.2167	5.7500	0	KNMI	3	No
Lerwick	UK	x	x	60.1333	-1.1833	84	Lerwick	3	No
Lindenberg	Germany	x	-	52.2100	14.1220	125	In. 2013 (BSRN)	4	No
Lleida	Spain	x	x	41.6258	0.5950	192	AEMET	2	No
Locarno-Monti	Switzerland	x	-	46.1726	8.7874	370	-	3	No
Longe	Zambia	x	x	-14.8397	24.9319	1167	ESMAP	3	Yes
Longreach	Australia	x	x	-23.4397	144.2828	192	BOM	2	Yes
Loughborough	United Kingdom	x	-	52.7700	-1.2300	70	Lgb. univ.	3	Yes
Lusaka	Zambia	x	x	-15.3946	28.3372	1262	ESMAP	3	Yes
M Bour	Senegal	x	-	14.3940	-16.9590	5	-	2	Yes
Maan	Jordan	x	x	30.1720	35.8183	1020	ENERMENA	2	Yes
Madison	Wisconsin, USA	x	x	43.0725	-89.4113	271	NOAA ISIS	4	Yes
Madrid	Spain	x	x	40.4528	-3.7242	664	AEMET	2	No
Malaga	Spain	x	x	36.7192	-4.4803	60	AEMET	3	No
Manah	Oman	x	x	22.6031	57.6672	345	OPWP	2	Yes
Manua Loa	Hawaii, USA	x	x	19.5362	-155.5763	3397	NOAA ESRL	5	No
Masrik	Armenia	x	x	40.2077	45.7645	1944	ESMAP	4	Yes
Melbourne	Australia	x	x	-37.6655	144.8321	113	BoM	3	Yes

Site name	Country	GHI	DNI	Latitude [°]	Longitude [°]	Elevation [m a.s.l.]	Source	Climate zone	Recently updated
Mildura	Australia	x	x	-34.2358	142.0867	50	BOM	2	Yes
Minamitorishima	Japan	x	x	24.2883	153.9833	7	BSRN	1	Yes
Misamfu	Zambia	x	x	-10.1726	31.2231	1382	ESMAP	3	Yes
Mochipapa	Zambia	x	x	-16.8382	27.0703	1282	ESMAP	3	Yes
Momote	Papua New Guinea	x	x	-2.0580	147.4250	6	BSRN	1	Yes
Mount Makulu	Zambia	x	x	-15.5483	28.2482	1224	ESMAP	3	Yes
Multan	Pakistan	x	x	30.1654	71.4978	123	ESMAP	2	Yes
Murcia	Spain	x	x	38.0028	-1.1694	62	AEMET	2	No
Mutanda	Zambia	x	x	-12.4236	26.2153	1317	ESMAP	3	Yes
Mysore	India	x	x	12.3710	76.5840	799	SRRA	2	Yes
Mzuzu	Malawi	x	x	-11.4199	33.9953	1285	ESMAP	3	Yes
Nairobi	Kenya	x	-	-1.3389	36.8653	1650	SolRad-net	3	Yes
Nantes	France	x	-	47.2542	-1.5536	30	IDMP	3	No
Nauru Island	Nauru	x	x	-0.5210	166.9167	7	BSRN	1	Yes
Oviedo	Spain	x	x	43.3536	-5.8733	336	AEMET	3	No
Palangkaraya	Indonesia	x	-	-2.2280	113.9460	27	SOLARFLUX	1	No
Palma	Spain	x	x	39.5667	2.7439	4	AEMET	2	No
Pampa Camarones	Chile	x	-	-18.8584	-70.2173	798	ministerio de energia	2	Yes
Pantnagar	India	x	-	29.0458	79.5208	241	SolRadNet	3	No
Payerne	Switzerland	x	x	46.8150	6.9440	491	BSRN	4	No
Peshawar	Pakistan	x	x	34.0017	71.4854	367	ESMAP	2	Yes
Petrolina	Brasil	x	x	-9.0680	-40.3190	387	BSRN	2	Yes
Port Elizabeth	South Africa	x	x	-34.0086	25.6653	33	SAURAN	2	Yes
Potsdam	Germany	x	-	52.3667	13.0833	107	DWD	4	No
Pozo Almonte	Chile	x	-	-20.2568	-69.7750	1033	ministerio de energia	2	Yes
Pretoria	South Africa	x	x	-25.7531	28.2286	1381	SAURAN	3	No
Puerto Angamos	Chile	x	-	-23.0736	-70.3856	28	ministerio de energia	2	Yes
Qassim	Saudi Arabia	x	x	26.3100	43.7700	647	KACST	2	No
Quetta	Pakistan	x	x	30.2708	66.9398	1586	ESMAP	2	Yes
Ranchi	India	x	x	23.4430	85.2550	738	SRRA	3	No
Regina	Canada	x	-	50.2050	-104.7128	588	SOLRADNET	4	Yes
Richtersveld	South Africa	x	x	-28.5608	16.7615	141	SAURAN	2	Yes
Rock Springs	Pennsylvania, USA	x	x	40.7201	-77.9309	376	SURFRAD	4	Yes
Rockhampton	Australia	x	x	-23.3753	150.4775	10	BoM	3	Yes
Rutland	Vermont, USA	x	x	43.6370	-72.9750	184	SURFRAD	4	Yes

Site name	Country	GHI	DNI	Latitude [°]	Longitude [°]	Elevation [m a.s.l.]	Source	Climate zone	Recently updated
Salar de	Chile	x	-	-22.3409	-68.8766	2521	ministerio energia	2	Yes
Salt Lake City	Utah, USA	x	x	40.7722	-111.9550	1228	NOAA ISIS	2	Yes
Salvador de	Chile	x	-	-26.3127	-69.7504	1609	ministerio energia	2	Yes
San Bartolome Tirajana	Canary Isl.	x	x	27.7581	-15.5756	50	AEMET	2	No
San Pedro de Atacama	Chile de	x	-	-22.9767	-68.1601	2379	ministerio energia	2	Yes
San Sebastian	Spain	x	x	43.3075	-2.0394	252	AEMET	3	No
Sao Martinho da Serra	Brasil	x	x	-29.4428	-53.8231	489	BSRN	3	Yes
Sapporo	Japan	x	x	43.0600	141.3283	17	BSRN	4	Yes
Schleswig	Germany	x	-	54.5181	9.5704	12	DWD	3	No
Seattle	Washington, USA	x	x	47.6869	-122.2567	20	NOAA ISIS	3	Yes
Sede Boqer	Israel	x	x	30.8667	34.7667	457	BSRN	2	No
Seoul Yonsei University	South Korea	x	-	37.5644	126.9349	88	SOLARFLUX	4	Yes
Sharurah	Saudi Arabia	x	-	17.4700	47.1100	725	KACST/NREL	2	No
Silpakorn	Thailand	x	-	13.8188	100.0408	72	SOLARFLUX	1	No
Sion	Switzerland	x	-	46.2200	7.3300	489	In. 2011 (ANETZ)	4	No
Sioux Falls	South Dakota, USA	x	x	43.7340	-96.6233	473	SURFRAD	4	Yes
SLF Versuchsfeld	Switzerland	x	-	46.8279	9.8094	2540	-	5	No
Solar Village	Saudi Arabia	x	x	24.9100	46.4100	650	BSRN	2	No
Song Binh	Vietnam	x	-	11.2641	108.3452	62	ESMAP	1	Yes
Soria	Spain	x	x	41.7667	-2.4667	1082	AEMET	3	No
Stellenbosch Sonbesie	South Africa	x	x	-	18.8651	122	SAURAN STERG	3	No
Sterling	Virginia, USA	x	x	38.9767	-77.4838	85	NOAA ISIS	3	Yes
Sutherland	South Africa	x	x	-32.2220	20.3479	1318	SAURAN	2	No
Tabouk	Saudi Arabia	x	x	28.3800	36.6100	768	KACST	2	No
Talin	Armenia	x	x	40.3860	43.8927	1641	ESMAP	4	Yes
Tamanrasset	Algeria	x	x	22.7833	5.5137	1378	BSRN	2	No
Tartu-Toravere	Estonia	x	x	58.2653	26.4661	70	BSRN	4	No
Tateno	Japan	x	x	36.0500	140.1333	25	BSRN	3	Yes
Tatouine	Tunisia	x	x	32.9741	10.4851	209	ENERMENA	2	Yes
Thessaloniki	Greece	x	-	40.6324	22.9591	60	WRDC	2	No
Touba	Senegal	x	-	14.7725	-15.9196	37	IFC	2	Yes
Townsville	Australia	x	x	-19.2483	146.7661	4	BOM	1	Yes

Site name	Country	GHI	DNI	Latitude [°]	Longitude [°]	Elevation [m a.s.l.]	Source	Climate zone	Recently updated
Trinidad Head Observatory	California, USA	x	x	41.0541	-124.1510	107	NOAA ESRL	3	Yes
Tucson	Arizona, USA	x	x	32.2296	-110.9553	786	NREL	2	Yes
USM Penang	Malaysia	x	-	5.3580	100.3020	51	solradnet	1	No
Val Alinya	Spain	x	-	42.1520	1.4490	1770	In. 2011 (FluxNet)	4	No
Valladolid	Spain	x	x	41.6500	-4.7667	735	AEMET	2	No
Vanrhynsdorp	South Africa	x	x	-31.6175	18.7383	130	SAURAN	2	Yes
Varennes	Canada	x	x	45.6300	-73.3800	20	SACC	4	Yes
Vaulx un Velin	France	x	x	45.7786	4.9225	170	IDMP	3	Yes
Venda	South Africa	x	x	-23.1310	30.4240	628	SAURAN	3	Yes
Vryheid	South Africa	x	x	-27.8282	30.5000	1274	SAURAN	3	No
Wadi Al-Dawaser	Saudi Arabia	x	x	20.4400	44.6800	701	KACST	2	No
Wagga	Australia	x	x	-35.1583	147.4573	212	BoM	2	Yes
Warangal	India	x	x	18.0750	79.7050	278	SRRA	1	No
Watkins	USA	x	x	39.7568	-104.6202	1674	NREL	2	Yes
Weihenstephan	Germany	x	x	48.4000	11.7000	472	-	4	No
Weissfluhjoch	Switzerland	x	-	46.8332	9.8053	2690	-	5	No
Westdorpe	Netherlands	x	-	51.2167	3.8667	2	KNMI	3	No
Wien	Austria	x	x	48.2485	16.3556	203	WRDC	4	No
Windhoek	Namibia	x	x	-22.5650	17.0750	1683	SAURAN	2	Yes
Woomera	Australia	x	x	-31.1558	136.8054	167	BOM	2	Yes
Wroclaw	Poland	x	-	51.1263	17.0138	111	IDMP	4	No
Xianghe	China	x	x	39.7540	116.9620	32	BSRN	4	No
Yerevan	Armenia	x	x	40.1887	44.3976	946	ESMAP	2	Yes
Zagreb	Croatia	x	-	45.8188	16.0129	119	-	3	No

GHI validation statistics

Site name	Country	Valid data pairs	Bias GHI		Root Mean Square Deviation GHI		
			[%]	[W/m2]	Hourly [%]	Daily [%]	Monthly [%]
A Coruna	Spain	7805	-1.6	-5	17.3	9.2	3.0
Abha	Saudi Arabia	13824	1.5	8.6	13.9	6.1	2.3
Adam	Oman	16979	-1.8	-10	9.3	6.1	3.8
Adelaide	Australia	38160	-1.6	-7	15.1	8	2.1
Aggeneys	South Africa	5886	-1.1	-6	8.8	3.6	1.4
Agoufu	Mali	3315	-1.1	-6	10.4	6.1	3.0
Al-Ahsa	Saudi Arabia	11725	-1.4	-7.3	10	6.7	2.6
Al-Jouf	Saudi Arabia	7027	1.8	9.2	9.9	6.1	2.8
Al-Madinah	Saudi Arabia	10883	3	15.8	11.8	7.1	3.7
Al-Qaisumah	Saudi Arabia	8609	-1.5	-7.8	9.8	6.1	1.9
Alamosa	Colorado, USA	6318	-4.6	-24	21	12.6	5.6
Albuquerque	New Mexico, USA	24267	0.9	5	14.7	6.7	1.4
Alice Springs	Australia	38048	0.8	4	12.1	5.8	1.1
Almeria PSA	Spain	19528	0.3	1	11.8	5.2	1.1
American Samoa Observatory	ASM	44032	-0.6	-3	21.2	9	0.9
Amman	Jordan	-	-1.9	-10	9.6	3.8	1.9
Armazones	Chile	12989	-3	-21	5.4	3.8	3.1
Athens	Greece	4068	2.4	10	15.1	8.1	3.2
BacNinh	Vietnam	3868	1.3	4	30.8	18.9	8.5
Badajoz	Spain	7946	1.4	6	11.6	5.5	2.3
Bahawalpur	Pakistan	8409	-1.6	-7	14.2	10.7	6.9
Bamba	Mali	4106	-2.3	-13	11.6	7.8	5.2
Banizoumbou	Niger	4129	-2.0	-11	12.1	7.5	4.9
Barcelona	Spain	2625	2.1	8	14.0	6.7	2.7
Bergen	Norway	3755	7.5	14	29.9	16.7	10.9
Bismarck	North Dakota, USA	25594	-0.9	-3	19.0	11.5	1.6
Bloemfontein	South Africa	11381	-0.8	-3	10.3	4.2	1.2
Bondville	Illinois, USA	67113	-1.4	-6	17.9	10.7	2.8
Boulder	Colorado, USA	68488	0.1	1	23.9	12.8	3.5
Bovoni 2, St. Thomas	Virgin Islands, USA	2416	2.9	15	28.2	15.8	5.2
Bozeman	Montana, USA	8434	-1.6	-6	21.8	11.3	2.5
Brasilia	Brasil	8690	3.4	17	19.6	8.3	4.7
Bratislava	Slovakia	3981	2.0	6	18.2	9.5	3.6
Broome	Australia	36637	0.8	5	11.5	6.1	2.2

Site name	Country	Valid data pairs	Bias GHI		Root Mean Square Deviation GHI		
			[%]	[W/m2]	Hourly [%]	Daily [%]	Monthly [%]
Bukit Kototabang	Indonesia	22593	0.6	2	31.6	14.8	2.5
Cabauw	Netherlands	11910	-2.5	-7	19.1	8.5	4.0
Caceres	Spain	4463	2.0	8	12.2	6.1	2.9
Camborne	UK	7108	-3.4	-10	18.8	8.9	4.3
Cape Grim	Australia	34782	-4.8	-18	20.2	10.9	5.4
Carpentras	France	31748	0.7	2.7	12.5	5.5	1.1
Cener	Spain	34263	0.9	3	16.2	7.4	2.0
Central Highlands	Vietnam	3948	-1.1	-5	21.3	9.1	4.2
Cerro Calan	Chile	14778	5.2	22	15.4	9	5.8
Chilanga	Malawi	6832	8.6	39	24.9	14.0	10.8
Chileka	Malawi	-	8.3	38	-	-	-
Cimetta	Switzerland	-	6.1	18	27.3	14.6	8
Cobar	Australia	6348	-0.3	-2	13.3	6.3	2.3
Copiapo	Chile	5064	-1.4	-7	14.3	7.5	2.1
Cordoba	Spain	4600	2.8	13	11.8	6.8	4.0
Crete_TEI	Greece	16006	0.9	4	12.8	6.5	1.7
Crucero2	Chile	23471	-1.9	-12	6.3	3.5	2
DaNang	Vietnam	3266	4	15	21.6	10.5	5.4
Dar es Salaam	Tanzania	5803	8.1	38	21.5	11.7	9.4
Darwin	Australia	37061	2.8	14	19.4	10.1	3
Davos	Switzerland	-	-3.7	-12	27.5	14	5.4
De Aar	South Africa	2344	2.1	11	10.7	6.6	3.0
Desert Rock	Nevada, USA	59165	-1.3	-8	13.8	6.7	2.2
Dicheto	Ethiopia	4062	-0.7	-4	10.9	5.6	3.0
Djougou	Benin	4154	2.6	12	16.4	9.6	5.5
Durban 1	South Africa	5756	-1.6	-6	17.2	8.6	3.3
Edinburg	Texas, USA	16485	-0.8	-3	15.3	6.3	1.0
Egbert	Canada	8633	-2.8	-10	20.9	11.5	3.7
Eggishorn	Switzerland	-	1.6	5	42.1	27	15.3
El Nido Airport	Philippines	686	-3.1	-13	26.4	10.7	5.7
El Saler	Spain	-	1	4	-	-	-
Ell	Netherlands	11973	0.0	0	17.7	7.8	2.2
Eugene	Oregon, USA	10070	0.4	1	18.9	9.2	1.4
Fatick	Senegal	4424	-1.9	-10	10.9	6.3	2.9
Feni	Bangladesh	5223	0.8	3	20.3	9.6	3.9
Florianopolis	Brasil	15300	-1.7	-6	21.5	9.5	2.0
Fort Peck	Montana, USA	54797	-0.2	-1	17.5	10.2	2
Freiburg	Germany	2726	4.1	14	19.0	8.6	4.6
Fukuoka	Japan	29983	1.6	6	19.9	10.5	2.6

Site name	Country	Valid data pairs	Bias GHI		Root Mean Square Deviation GHI		
			[%]	[W/m2]	Hourly [%]	Daily [%]	Monthly [%]
Gaborone	Botswana	7104	2.5	13	11.4	5.5	3.1
Gan	Maldives	8311	1	5	15.7	6.8	1.7
Ganovce	Slovakia	25654	-2.6	-8	24.1	12.0	3.4
Geneve	Switzerland	17081	4.5	14	18.8	9.4	4.7
Geraldton	Australia	8251	-1.2	-6	12.8	6.2	1.5
Gizan	Saudi Arabia	14522	-1.3	-6.7	10.9	6.6	2.8
Gobabeb	Namibia	20740	-1.4	-8	7.1	4.2	1.9
Goodwin Creek	Mississippi, USA	63228	1.5	6	14.8	6.8	1.9
Gornergrat	Switzerland	-	-6.6	-25	31.1	19.3	11.2
Gospic	Croatia	-	1.2	3	24.7	11.1	3.2
Graaff-Reinet	South Africa	2975	0.6	3	11.6	4.9	1.0
Hamburg	Germany	-	1.6	3	20.8	9.5	3.3
Hanford	California, USA	32351	0.8	4	10.7	5.4	1.2
Hanimaadhoo	Maldives	8354	0.8	4.1	15.4	6.8	2.6
Heino	Netherlands	12053	-1.0	-2	19.5	8.3	3.0
Helios	South Africa	5420	-1.1	-6	9.5	3.8	1.4
Hradec Kralove	Czech republic	11532	0.5	1	21.3	10.2	3.3
Hrazdan	Armenia	3968	-5.2	-22.3	28	16.8	11.5
Hulhulé	Maldives	8294	-0.1	-0.4	16.5	7.2	1.8
Hurso	Ethiopia	4174	2.8	15	14.8	6.5	3.4
Hyderabad	Pakistan	7059	-3.7	-20	9.8	6.7	5.1
Ilorin	Nigeria	4685	7.7	34	22.8	13.8	10.5
Inca de Oro	Chile	30396	-1.6	-10	6.2	3.4	1.8
Ishigakijima	Japan	30450	0.2	1	20.4	10.6	1.4
Islamabad	Pakistan	8980	3.3	13	15.3	8.7	3.8
Ispra	Italy	-	4.6	13	15.4	7.7	4.8
Izana	Canary Isl.	5272	-8.8	-51	18.1	13.1	9.3
Jaipur	India	5668	2.6	12.2	14.3	9.8	6.1
Jungfraujoch	Germany	-	-1.3	-5	32.7	20.8	11.5
Kadhdhoo	Maldives	8228	0.6	3.3	16.5	6.8	1.1
Kahone	Senegal	4072	-1.2	-7	10.8	6.4	2.8
Kailua-Kona	Hawaii, USA	3999	0.2	1	13	5	1.5
Kalgoorlie-Boulder	Australia	7053	-0.2	-1	12.9	6.3	1.9
Kanpur	India	16262	-2	-8.7	15.1	8.2	2.6
Karachi	Pakistan	7243	0.3	1	10.7	6.6	4.6
Kasungu	Malawi	7396	5.3	26	19.8	9.7	6.5
Keeling	Cocos Islands	37298	-2.8	-14	20.5	9.9	3.4
Khuzdar	Pakistan	5464	-1.2	-6	11.7	6.4	2.6
Kishinev	Moldova	15297	-0.2	-1	16.5	8.1	1.9

Site name	Country	Valid data pairs	Bias GHI		Root Mean Square Deviation GHI		
			[%]	[W/m2]	Hourly [%]	Daily [%]	Monthly [%]
Kosrae	Micronesia	2593	5.6	21	35	15.4	6.7
Kwajalein	Micronesia	14724	-2	-9	17.3	7.9	2.2
Lafayette	Louisiana, USA	2830	0.3	1	15.9	6.0	1.4
Lahore	Pakistan	8862	3.7	15	16.7	11.6	5.6
Lauder	New Zealand	35027	-4	-14	29.6	15.7	5.3
Learmonth	Australia	7675	-0.4	-2	9.3	4.4	1.3
Leeuwarden	Netherlands	11969	-1.4	-4	18.8	8.6	3.0
Lerwick	UK	6526	0.3	1	26.9	14.5	4.1
Lindenberg	Germany	-	-3	-9	-	-	-
Lleida	Spain	6190	-1.8	-7	12.6	7.3	3.9
Locarno-Monti	Switzerland	-	-0.3	-1	17.7	7.9	2.1
Longe	Zambia	8369	6.6	33	18.4	10.3	8.7
Longreach	Australia	5262	0.2	1	11.7	5.5	1.2
Loughborough	United Kingdom	3495	-1.3	-3	22.9	11.8	3.7
Lusaka	Zambia	8935	6.8	32	19.1	10.4	8.6
M Bour	Senegal	3167	1.9	10	11.0	6.4	3.3
Maan	Jordan	19387	-1.2	-6.8	8.7	4.2	1.6
Madison	Wisconsin, USA	34201	-1.8	-6	16.8	9.1	2.5
Madrid	Spain	8107	1.2	5	12.8	6.5	1.8
Malaga	Spain	7071	1.9	8	14.0	7.1	2.7
Manah	Oman	23059	-1.9	-10	10.8	6.8	4.6
Manua Loa	Hawaii, USA	49774	-6.7	-40	16.8	10.1	6.9
Masrik	Armenia	3701	-7.7	-33.1	28.6	17.5	12
Melbourne	Australia	35599	-2.8	-11	21.5	10.8	3.7
Mildura	Australia	3957	-1.6	-8	14	7.2	2.9
Minamitorishima	Japan	30439	0.2	1	13.3	5.8	0.9
Misamfu	Zambia	8639	6.4	32	19.8	9.9	7.9
Mochipapa	Zambia	8894	5.4	26	18.4	9.1	7.1
Momote	Papua New Guinea	25051	-2.9	-13	25.9	12.4	3.8
Mount Makulu	Zambia	8886	6.4	30	21.2	11.0	9.0
Multan	Pakistan	9001	3.1	13	13.7	9.6	5.7
Murcia	Spain	7852	0.1	0	11.8	5.7	1.5
Mutanda	Zambia	8574	9.5	46	21.8	12.6	11.2
Mysore	India	4144	2.5	12	16.5	8.2	5
Mzuzu	Malawi	7158	12.3	58	25.5	15.8	12.8
Nairobi	Kenya	-	2	10	18	7.3	3.5
Nantes	France	15008	-2.4	-8	17.9	9.8	3.2
Nauru Island	Nauru	9050	3.1	16	20	10.5	3.5

Site name	Country	Valid data pairs	Bias GHI		Root Mean Square Deviation GHI		
			[%]	[W/m2]	Hourly [%]	Daily [%]	Monthly [%]
Oviedo	Spain	7739	6.5	19	23.2	13.4	7.0
Palangkaraya	Indonesia	356	-4.6	-20	21.7	9.8	8
Palma	Spain	6443	-1.9	-8	13.3	5.9	2.2
Pampa Camarones	Chile	31083	-0.3	-2	9.3	4.1	0.7
Pantnagar	India	616	-1.2	-5.25	17.4	11.4	2.5
Payerne	Switzerland	18840	0.6	2	17.6	8.9	1.9
Peshawar	Pakistan	7125	4.6	19	14.6	9.5	5.6
Petrolina	Brasil	7174	2.9	15	18.0	8.3	3.4
Port Elizabeth	South Africa	9982	-2.8	-12	13.1	6.6	3.3
Potsdam	Germany	7849	-2.7	-7	17.7	8.6	4.0
Pozo Almonte	Chile	17590	-1	-6	7.2	3.6	1.7
Pretoria	South Africa	3685	1.4	7	14.6	6.1	1.9
Puerto Angamos	Chile	13007	0.5	3	9.6	4.7	1.5
Qassim	Saudi Arabia	14093	0.6	3.1	9.5	5.7	1.3
Quetta	Pakistan	5179	0.1	1	11.8	6.1	2.6
Ranchi	India	4004	3.8	18	13.9	7.7	5.2
Regina	Canada	25022	-2.3	-8	23.1	14.6	7.8
Richtersveld	South Africa	10495	0.0	0	7.5	3.7	1.0
Rock Springs	Pennsylvania, USA	63430	-0.4	-1	19.8	10.5	2
Rockhampton	Australia	32081	0.2	1	16.8	8.1	1.1
Rutland	Vermont, USA	3722	-1.2	-5	19.7	9.7	4.5
Salar	Chile	6516	2.2	14	8.4	4.2	2.3
Salt Lake City	Utah, USA	30065	-0.8	-4	17.3	8.1	2.1
Salvador	Chile	10029	-0.5	-3	4.6	2.6	1.1
San Bartolome Tirajana	Canary Isl.	1881	-0.7	-3	13.2	5.7	1.1
San Pedro de Atacama	Chile	14630	1.5	9	8.7	4.1	1.7
San Sebastian	Spain	6387	0.1	0	18.5	8.1	2.7
Sao Martinho da Serra	Brasil	30044	0.7	3	16.6	7.1	1.3
Sapporo	Japan	29748	-0.8	-2	25.4	13.7	1.8
Schleswig	Germany	3951	-4.5	-12	21.0	12.5	7.8
Seattle	Washington, USA	26158	2.7	8	21.3	9.8	3.7
Sede Boqer	Israel	12341	0.7	3.6	16.5	7.4	2.7
Seoul Yonsei University	South Korea	16377	2.7	10	17.9	9.6	3.4
Sharurah	Saudi Arabia	-	-0.5	-3	9.6	5.5	1.9
Silpakorn	Thailand	7308	-1.9	-9	23.6	12.2	5

Site name	Country	Valid data pairs	Bias GHI		Root Mean Square Deviation GHI		
			[%]	[W/m2]	Hourly [%]	Daily [%]	Monthly [%]
Sion	Switzerland	-	-3	-11	-	-	-
Sioux Falls	South Dakota, USA	49420	-1.8	-7	17.6	11	3
SLF Versuchsfeld	Switzerland	-	-2.4	-7	32.2	18	9
Solar Village	Saudi Arabia	23206	-0.7	-3.8	8.5	4.7	1.3
Song Binh	Vietnam	3630	3.5	17	17.4	8	4.6
Soria	Spain	6656	-1.1	-4	17.6	7.4	1.8
Stellenbosch Sonbesie	South Africa	13981	-0.5	-2	10.4	4.5	1.5
Sterling	Virginia, USA	34550	1.4	5	17.0	8.4	2.2
Sutherland	South Africa	7239	-1.6	-9.0	10.7	4.6	1.9
Tabouk	Saudi Arabia	9699	5	26.6	10.8	7.6	5.3
Talin	Armenia	3898	-3	-13.2	21.5	12.8	7.4
Tamanrasset	Algeria	10019	-0.9	-5.8	8.5	4.8	2.2
Tartu-Toravere	Estonia	11109	-1.9	-5	22.7	11.8	4.9
Tateno	Japan	40564	-0.2	-1	18.6	9.3	2.1
Tatouine	Tunisia	17548	-2.5	-13	9.7	5.7	2.7
Thessaloniki	Greece	10401	-0.1	0	13.0	6.0	1.7
Touba	Senegal	4074	-2.5	-13	10.2	6.4	3.6
Townsville	Australia	7038	0	0	13.8	6	0.7
Tri An	Vietnam	4009	-1.4	-7	18.9	8.1	5
Trinidad Head Observatory	California, USA	20211	0.5	2	18	8.9	1.9
Tucson	Arizona, USA	29874	-0.5	-3	12.7	5.1	0.9
USM Penang	Malaysia	942	5.8	22.9	32.3	13.7	6.9
Val Alinya	Spain	-	2	9	-	-	-
Valladolid	Spain	7973	2.5	10	13.4	6.7	3.2
Vanrhynsdorp	South Africa	14881	0.2	1	8.2	3.4	0.8
Varennes	Canada	7882	-2.9	-10	18.1	9.0	4.3
Vaulx un Velin	France	14597	5.5	17	16.2	9.0	5.8
Venda	South Africa	12720	0.7	3	15.1	7.3	2.8
Vryheid	South Africa	3483	0.7	3	14.3	5.9	2.4
Wadi Al-Dawaser	Saudi Arabia	12512	1.2	6.7	10.5	6.2	1.7
Wagga	Australia	36210	-1.7	-8	16.6	8.8	2.7
Warangal	India	5251	4.7	22	14.5	9.8	7.3
Watkins	USA	25801	-2.9	-13	19.2	11.5	4.1
Weihenstephan	Germany	-	-2.3	-6	20.4	10.1	3.7
Weissfluhjoch	Switzerland	-	-2.8	-9	31.5	18	8.9
Westdorpe	Netherlands	11912	1.4	4	19.0	8.7	2.4
Wien	Austria	15347	1.5	4	19.4	9.3	2.7

Site name	Country	Valid data pairs	Bias GHI		Root Mean Square Deviation GHI		
			[%]	[W/m2]	Hourly [%]	Daily [%]	Monthly [%]
Windhoek	Namibia	4359	2.3	12	15.0	6.5	3.3
Woomera	Australia	4343	0.4	2	12.2	5.9	2.1
Wroclaw	Poland	3900	1.7	5	18.3	8.4	3.1
Xianghe	China	14891	-1	-3	19.9	14.5	3.9
Yerevan	Armenia	3888	1.5	6.1	18.1	10.3	5.3
Zagreb	Croatia	-	1.7	5	19.2	8.1	3.2

DNI validation statistics

Site name	Country	Valid data pairs	Bias DNI		Root Mean Square Deviation DNI		
			[%]	[W/m2]	Hourly [%]	Daily [%]	Monthly [%]
A Coruna	Spain	6300	3.8	12	31.2	17.4	5.3
Abha	Saudi Arabia	13724	-0.2	-1.4	22.2	12.7	3.4
Adam	Oman	12813	-6	-32	19.7	15.1	8.3
Adelaide	Australia	37586	2.9	14	29.7	15.9	4.2
Aggeneys	South Africa	5743	1.6	12	14.6	8.6	2.4
Al-Ahsa	Saudi Arabia	11695	1.4	6.9	26.7	20.2	6.6
Al-Jouf	Saudi Arabia	7011	0.8	4.5	20.9	14.7	5.6
Al-Madinah	Saudi Arabia	10862	0.6	3.4	20	13.9	4.7
Al-Qaisumah	Saudi Arabia	8574	-4.8	-24.5	22.8	18.2	9.4
Alamosa	Colorado, USA	6318	2.2	14	30.2	17.1	3.9
Albuquerque	New Mexico, USA	21947	5.8	39	25.1	14.7	6.9
Alice Springs	Australia	3605	3.3	22	20.5	11.6	3.8
Almeria PSA	Spain	18438	-3.2	-18.1	22.0	13.0	4.3
American Samoa Observatory	ASM	43737	-4.1	-17	42.2	19.9	4.8
BacNinh	Vietnam	3723	5.1	7	73.4	44.5	15.3
Badajoz	Spain	3646	9.0	42	26.8	18.7	9.6
Bahawalpur	Pakistan	7457	-7.1	-27	27.9	22.3	13.3
Bismarck	North Dakota, USA	22030	1.9	7	37.3	22.9	6.2
Bloemfontein	South Africa	11381	1.7	11	16.9	9.1	3.0
Bondville	Illinois, USA	65367	2.7	10	34.2	21.1	4
Boulder	Colorado, USA	66302	4.9	25	40.1	23.2	5.4
Brasilia	Brasil	7673	4.1	21	29.9	14.7	5.5
Broome	Australia	35318	1.4	9	20	11.4	2.9
Bukit Kototabang	Indonesia	15301	8.9	19	72.6	42.1	11
Cabauw	Netherlands	-	-6	-13	-	-	-
Caceres	Spain	3106	3.4	16	26.0	15.6	8.0
Camborne	UK	7108	1.0	2	41.3	22.6	6.7
Cape Grim	Australia	32695	0.5	2	45.8	24.1	3.6
Carpentras	France	31748	-0.9	-4.2	24.7	14.8	6.2
Cener	Spain	34239	1.9	7	32.8	19.1	7.8
Central Highlands	Vietnam	3948	3.3	10	46.2	22.3	6.5
Chilanga	Malawi	6818	10.7	43	39.0	21.6	14.7
Chileka	Malawi	-	10.5	42	-	-	-
Cobar	Australia	6279	2.4	16	22.1	11.3	4.4
Cordoba	Spain	2292	11.7	46	33.6	22.9	13.6

Site name	Country	Valid data pairs	Bias DNI		Root Mean Square Deviation DNI		
			[%]	[W/m2]	Hourly [%]	Daily [%]	Monthly [%]
Crucero2	Chile	23105	-7.6	-64	16.4	12.5	8.2
Dar es Salaam	Tanzania	5671	16.1	57	43.4	25.2	20.7
Darwin	Australia	34993	2.2	10	29.4	14.7	3.2
Davos	Switzerland	-	7.2	21	58.7	27	10.2
De Aar	South Africa	2344	3.3	23	15.5	9.5	4.0
Desert Rock	Nevada, USA	58675	0	0	22.6	13.4	4.5
Dicheto	Ethiopia	4169	-1.7	-8	22.6	14.8	10.6
Durban 1	South Africa	5756	0.5	2	28.3	13.7	2.2
Edinburg	Texas, USA	16509	4.1	15	29.8	15.8	5.8
Egbert	Canada	8631	9.1	29	48.4	30.1	12.1
Eugene	Oregon, USA	10052	0.4	1	37.9	19.3	5.2
Feni	Bangladesh	5223	-4.6	-12	40.9	23	10.6
Florianopolis	Brasil	14358	-2.0	-6	40.6	19.7	3.8
Fort Peck	Montana, USA	53542	0.4	2	35.3	20.8	6.3
Freiburg	Germany	2738	2.9	9	36.4	17.0	7.1
Fukuoka	Japan	29927	0.8	2	40.6	23	4.4
Gaborone	Botswana	7104	2.8	17	19.0	10.7	3.7
Gan	Maldives	7139	7.3	28.9	34.5	19.3	8.5
Geneve	Switzerland	17081	8.6	27	39.8	23.9	11.2
Geraldton	Australia	8229	2.8	16	23	12.8	5.2
Gizan	Saudi Arabia	14408	-6.9	-29.6	24.2	18	11.2
Gobabeb	Namibia	2069	-6.4	-46	16.6	11.7	6.8
Goodwin Creek	Mississippi, USA	61769	2.9	12	27.2	16	3.6
Graaff-Reinet	South Africa	2975	0.8	4	20.1	9.7	2.3
Hamburg	Germany	-	-9.3	-31	32.3	22.8	14.1
Hanford	California, USA	31240	3.2	18	21.6	13.4	4.6
Hanimaadhoo	Maldives	8081	5.3	19.3	32.3	18	7.3
Helios	South Africa	8478	1.3	9	17.1	10.5	2.5
Hradec Kralove	Czech republic	12031	0.5	1	42.8	25.6	13.1
Hrazdan	Armenia	3968	-9.6	-43.4	57.2	40.9	27.3
Hulhule	Maldives	-	6	22	35.5	19.7	7.4
Hulhulé	Maldives	7797	8.1	29.9	35.8	20.3	8.8
Hurso	Ethiopia	3634	2.3	11	25.3	14.3	8.6
Hyderabad	Pakistan	7287	-2.5	-11	24.7	17.5	5.1
Ishigakijima	Japan	30015	5.4	14	45	24.6	6.6
Islamabad	Pakistan	7793	1.1	4	29.7	20.7	4.6
Izana	Canary Isl.	4621	-10.4	-74	31.4	24.8	12.9
Kadhdhoo	Maldives	7518	7	26.7	35.6	19.2	7.4
Kalgoorlie-Boulder	Australia	6886	7.9	45	24.6	14.2	9.6

Site name	Country	Valid data pairs	Bias DNI		Root Mean Square Deviation DNI		
			[%]	[W/m2]	Hourly [%]	Daily [%]	Monthly [%]
Karachi	Pakistan	7279	4.9	17	27	18.6	7.7
Kasungu	Malawi	7384	8.1	36	34.7	18.2	10.3
Keeling	Cocos Islands	35625	-1.8	-7	46.3	21.3	4.7
Khuzdar	Pakistan	5464	-0.5	-3	22.3	15.5	6.7
Kishinev	Moldova	15048	-5.8	-20	33.7	21.5	13.4
Kwajalein	Micronesia	13290	-2.6	-10	34.8	16.8	3.4
Lafayette	Louisiana, USA	2828	6.5	21	30.5	16.7	7.9
Lahore	Pakistan	8881	3.8	11	35	26.2	9.6
Lauder	New Zealand	34782	5.8	23	51.5	27	7
Learmonth	Australia	7357	-1.1	-8	17.5	9.5	4
Lerwick	UK	6526	10.6	15	77.6	44.3	16.9
Lindenberg	Germany	-	-6	-19	-	-	-
Lleida	Spain	1052	-0.9	-3	30.9	20.7	10.5
Locarno-Monti	Switzerland	-	-4.5	-14	48.9	30.4	6.9
Longe	Zambia	8423	6.9	32	30.9	18.3	13.7
Longreach	Australia	4875	-0.6	-4	19.8	10.4	3.9
Lusaka	Zambia	8935	10.5	44	32.3	18.2	14.6
Maan	Jordan	19388	0	0.1	17.4	10.9	2.3
Madison	Wisconsin, USA	32844	2.8	10	34.4	21.0	3.8
Madrid	Spain	8095	0.0	0	23.1	14.1	5.3
Malaga	Spain	1781	8.8	37	30.8	23.0	10.3
Manah	Oman	15197	-3.9	-20	19.9	14.9	7.5
Manua Loa	Hawaii, USA	49433	-8.2	-63	24.4	15.2	8.5
Masrik	Armenia	3701	-15.9	-76.3	55.1	40.6	29.1
Melbourne	Australia	34451	5	18	41.4	21.3	5.8
Mildura	Australia	3737	1.5	8	25.9	13.3	5.8
Minamitorishima	Japan	3040	4.3	19	28	13.8	4.5
Misamfu	Zambia	8580	10.1	44	35.3	19.2	14.2
Mochipapa	Zambia	8936	9.0	41	30.4	17.1	12.6
Momote	Papua New Guinea	25057	3.1	10	51.6	24.4	5.8
Mount Makulu	Zambia	8863	9.9	42	34.8	19.5	14.9
Multan	Pakistan	9001	6.9	22	31.5	24.6	13.9
Murcia	Spain	6464	0.9	4	24.9	16.0	6.9
Mutanda	Zambia	8674	10.5	43	36.0	20.9	16.5
Mysore	India	5619	-0.2	-0.9	25.2	18.3	11.2
Mysore	India	3449	13.8	42	38.7	25.3	19.8
Mzuzu	Malawi	7231	18.4	73	43.2	26.9	20.0
Nantes	France	-	-8	-24	-	-	-

Site name	Country	Valid data pairs	Bias DNI		Root Mean Square Deviation DNI		
			[%]	[W/m2]	Hourly [%]	Daily [%]	Monthly [%]
Nauru Island	Nauru	8853	6.5	30	38.6	21.2	6.8
Oviedo	Spain	6367	7.8	22	47.9	26.9	11.5
Palma	Spain	3702	-2.3	-10	27.7	16.9	8.6
Payerne	Switzerland	15654	5.0	20	34.6	22.8	10.2
Peshawar	Pakistan	7125	0.1	0	31.9	24.6	10.1
Petrolina	Brasil	6004	8.9	42	35.9	18.6	10.4
Port Elizabeth	South Africa	7482	0.1	1	25.8	13.2	2.1
Pretoria	South Africa	3685	1.8	9	23.4	11.1	3.3
Qassim	Saudi Arabia	14063	-0.5	-2.7	21.2	15.8	6.1
Quetta	Pakistan	5526	5	28	24.5	17	11.7
Ranchi	India	4003	4.4	15	28.1	18.7	9.5
Richtersveld	South Africa	10388	-0.2	-1	15.8	9.6	2.0
Rock Springs	Pennsylvania, USA	60235	5.2	17	42	25.8	6.9
Rockhampton	Australia	30993	5.4	26	29.9	15.6	6
Rutland	Vermont, USA	3650	7.8	26	47.1	29.7	16.2
Salt Lake City	Utah, USA	28826	-2.9	-15	31.3	18.1	5.9
San Bartolome Tirajana	Canary Isl.	1571	1.3	6	26.7	16.0	2.3
San Sebastian	Spain	5454	1.8	5	36.4	19.6	6.2
Sao Martinho da Serra	Brasil	15227	1.4	7	27.4	13.2	2.6
Sapporo	Japan	29511	6.4	16	60.1	34.9	10.3
Seattle	Washington, USA	20907	6.1	18	39.4	20.6	7.3
Sede Boqer	Israel	12342	-3.6	-22	27.5	16.8	4.7
Sioux Falls	South Dakota, USA	47934	1.6	6	33.5	21	3.9
Solar Village	Saudi Arabia	22504	-1.8	-10.9	18.1	12.4	4.8
Soria	Spain	1116	3.9	14	31.6	17.4	8.3
Stellenbosch Sonbesie	South Africa	13981	1.0	5	23.5	16.6	3.1
Sterling	Virginia, USA	27493	3.9	14	35.4	21.2	6.0
Sutherland	South Africa	7135	1.8	12	17.2	9.1	2.5
Tabouk	Saudi Arabia	9678	8	50.1	20.5	14.8	9.2
Talin	Armenia	3898	-3.3	-15.6	41.4	28.5	11.7
Tamanrasset	Algeria	10019	1.2	7.7	21.0	15.9	4.2
Tartu-Toravere	Estonia	11109	-5.4	-15	48.1	31.3	16.9
Tateno	Japan	40566	-0.3	-1	36	20	2.8
Tatouine	Tunisia	17548	-7.6	-42	24.9	17.7	8.8
Townsville	Australia	6756	6.3	32	28.8	15.5	7.6

Site name	Country	Valid data pairs	Bias DNI		Root Mean Square Deviation DNI		
			[%]	[W/m2]	Hourly [%]	Daily [%]	Monthly [%]
Tri An	Vietnam	4009	2.2	7	38.9	20.5	12.3
Trinidad Head Observatory	California, USA	20081	10	29	48	26.3	16.5
Tucson	Arizona, USA	30440	3.9	25	21.6	12.0	5.6
Valladolid	Spain	7659	7.6	35	27.7	17.0	9.6
Vanrhynsdorp	South Africa	14881	0.8	5	16.2	9.7	1.5
Varennes	Canada	7783	2.4	8	41.6	24.9	6.4
Vaulx un Velin	France	9144	0.4	1	31.8	19.8	8.4
Venda	South Africa	12720	2.3	10	23.4	11.8	3.3
Vryheid	South Africa	3483	1.4	7	23.3	11.9	2.2
Wadi Al-Dawaser	Saudi Arabia	12500	-1.9	-10.6	22.4	16	3.9
Wagga	Australia	35543	2.1	11	29.4	16.2	4.5
Warangal	India	4668	10.6	35	30.7	23.3	16.6
Watkins	USA	25488	1.8	10	32.4	19.2	3.4
Weihenstephan	Germany	-	-4.3	-15	38	23.1	9.3
Wien	Austria	-	-2	-6	-	-	-
Windhoek	Namibia	4351	6.5	41	22.9	12.5	7.4
Woomera	Australia	4253	3.1	19	24	13.4	6.5
Xianghe	China	12880	1.9	6	45	36.4	5.9
Yerevan	Armenia	4123	-0.1	-0.2	39.7	28.9	17.3

SOLARGIS